AN OPTIMAL CONTROL FRAMEWORK FOR COORDINATION OF CONNECTED AND AUTOMATED VEHICLES WITH NOISY OBSERVATIONS AND DELAYED COMMUNICATION

by

Behdad Chalaki

Spring 2020

© 2020 Behdad Chalaki
All Rights Reserved

TABLE OF CONTENTS

LIST OF TABLES . . . . . **v**
LIST OF FIGURES . . . . . **vi**

Chapter

1 INTRODUCTION AND LITERATURE REVIEW **1**

1.1 Motivation 1
1.2 Coordination of connected and automated vehicles 2

1.2.1 Control of CAVs under uncertainty 4
1.2.2 Research gaps 7

2 PRELIMINARY RESULTS **8**

2.1 Hierarchical Optimal Coordination Framework for Connected and Automated Vehicles in Multiple Intersections 8

2.1.1 Problem Formulation 9
2.1.2 Modeling Framework 9
2.1.3 CAV model and assumptions 11
2.1.4 Upper-level Problem: Scheduling 13
2.1.5 Low-level problem: Energy Minimization 16
2.1.6 Solution of low-level and upper-level problems 16
2.1.7 Analytical solution of the release time and the deadline 17

2.1.7.1 State constraints are not active 18
2.1.7.2 State constraints are active 21

2.1.8 Solution of the scheduling problem (Problem 2.1.10) 27

2.1.9 Analytical solution of the energy minimization problem (Problem 2.1.12) . . . 27

2.1.9.1 State and control constraints are not active . . . 28
2.1.9.2 CAV travels on different constrained arcs . . . 29
2.1.9.3 CAV travels on the combination of constrained and unconstrained arc . . . 32
2.1.9.4 CAV enters the safety constrained arc . . . 33

2.1.9.4.1 Hamiltonian analysis when only rear-end safety is active . . . 35

2.1.10 Simulation results . . . 36

2.2 Experimental Validation of a Real-Time Optimal Controller for Coordination of CAVs in a Multi-Lane Roundabout . . . 39

2.2.1 Problem Formulation . . . 39
2.2.2 CAV Model and Constraints . . . 41
2.2.3 Analytical solution . . . 47
2.2.4 Experimental Setup . . . 50
2.2.5 Results and Discussion . . . 53

3 PROPOSED DISSERTATION RESEARCH . . . 59

3.1 Research plan . . . 60

4 EXPECTED CONTRIBUTIONS . . . 66

APPENDIX A PUBLICATIONS . . . 71

APPENDIX B COURSEWORK . . . 72

APPENDIX C CURRICULUM VITAE . . . 73

BIBLIOGRAPHY . . . 78

LIST OF TABLES

2.1 Computed Schedules for sixteen CAVs 37

2.2 Parameters used for the optimal controller in University of Delaware's scaled smart city; values are given in the 1:25 city scale. 53

2.3 Average velocity and travel time results for the 5 experiments. RMSE is normalized by travel time for each CAV. 53

4.1 A provisional timetable from Spring 2020 - Fall 2020 68

4.2 A provisional timetable from Winter 2020 - Winter 2021 69

4.3 A provisional timetable from Winter 2020 - Winter 2021 70

B.1 List of coursework 72

LIST OF FIGURES

2.1 Two interconnected intersections with a drone as a coordinator. . . 10

2.2 Zones numbered topologically and the fixed path for each CAV is shown. 11

2.3 Relative Position of CAV 2 and CAV 3 in zones which rear-end collision may occur. 38

2.4 Control input profile of CAV 15 for zones 10 and 3. 39

2.5 Control input profile of CAV 13 for zones 22 and 5. 40

2.6 Speed profile of CAV $13 - 16$ 41

2.7 Relative Position of CAVs travelling in zone 13. 42

2.8 A schematic of the roundabout scenario. The highlighted control zone continues upstream from the roundabout. There are three conflict points which may result in lateral collisions. 43

2.9 The University of Delaware's scaled smart city. The roundabout used in this experiment is in the upper-left side of the image. 51

2.10 A picture of the connected and automated vehicles in University of Delaware's scaled smart city. 52

2.11 Estimated and actual arrival time for each CAV over all experiments. The grey bar shows the range of admissible t_i^f from the state and control constraints. Every 9 CAVs corresponds to a single experiment; they are sorted in ascending order by departure time from the control zone. 54

2.12 Position trajectory for the third CAV entering from path 2 in the 5th experiment. The lateral constraints are shown as vertical lines, and the rear-end safety constraint is the hashed region. 55

2.13 Maximum, minimum, and average speed of CAVs on the path 1 (Fig.2.8) over the control zone length for the five experiments. . . . 56

2.14 Maximum, minimum, and average speed of CAVs on the path 2 (Fig.2.8) over the control zone length for the five experiments. . . . 57

2.15 Maximum, minimum, and average speed of CAVs on the path 3 (Fig.2.8) over the control zone length for the five experiments. . . . 58

3.1 Single intersection with control zone and a drone acting as a coordinator 61

Chapter 1

INTRODUCTION AND LITERATURE REVIEW

1.1 Motivation

Due to the increasing population and travel demand, traffic congestion has become a significant concern in big metropolitan areas. By 2050, it is expected that 66% of the population will reside in urban areas; by 2030, there would be 41 Mega-cities (with more than 10M people or more) [1]. Over the last decade, people in large urban areas across the US have experienced the negative effects of traffic congestion on their daily life. Schrank et al. [2] reported that congestion is persistently growing. In 2017, traffic congestion in urban areas in the US caused drivers to spend an extra 8.8 billion hours on the road, purchasing an extra 3.3 billion gallons of fuel for a congestion cost of $166 billion. In addition, traffic congestion has a negative impact on traffic safety, in 2018, there were 6M traffic accidents in the US resulting in more than 35K fatalities and 2.5M people injured; see [3]. Singh [4] reported that the immediate reason for 94% of the crashes was assigned to the driver, with recognition errors accounted for about 41%, decision errors 33 % and performance errors 11% of the crashes.

An automated transportation system [5] can alleviate congestion, reduce energy use and emissions, and improve safety significantly by the integration of information and communication technologies with cities. The use of connected and automated vehicles (CAVs) can transition our current transportation networks into energy-efficient mobility systems. The introduction of CAVs into the transportation system allows vehicles to make better operational decisions, leading to significant reductions of energy consumption, greenhouse gas emissions, and travel delays along with improvements to

passenger safety [6–9]. The generation of massive amounts of vehicle data also creates significant opportunities to develop optimization algorithms for controlling large-scale behaviors for the entire urban transportation system.

1.2 Coordination of connected and automated vehicles

CAVs have been used to improve both safety and efficiency of the transportation network using two primary approaches. In the first approach, which gained momentum in the 1980s and 1990s, CAVs are used to reduce vehicle gaps and form high-density platoons to cut congestion [10, 11]. In the second approach, CAVs are used to smooth the traffic flow to eliminate stop-and-go driving through optimal coordination at different traffic scenarios, e.g., merging at roadways, intersections, roundabouts, speed reductions zone [12]. Several research efforts have been reported in the literature on coordination of CAVs [13].

A series of papers have proposed a decentralized optimal control framework for coordinating online CAVs in such transportation scenarios. The analytical solution without considering state and control constraints, was presented in [14–16] for coordinating online CAVs at highway on-ramps, in [17] at two adjacent intersections, in [18] at roundabouts and in [19, 20] at a corridor. The solution of the unconstrained problem was also validated experimentally at University of Delaware's scaled smart city using 10 CAV robotic cars in [21] for a merging roadway scenario, in [22] at a corridor and in [23] at a multi-lane roundabout. The solution of the optimal control problem considering state and control constraints was presented in [24] at an urban intersection without considering rear-end collision avoidance constraint. In sequel papers, Malikopoulos and Zhao [25] enhanced the decentralized framework for a single intersection by including speed-dependent rear-end safety constraint. The conditions under which state and control constraints become active were explored in [26], and the conditions under which the rear-end collision avoidance constraint never becomes active were discussed in [27]. A

different approach has been explored in [28] and [29], in which the upper-level optimization problem yield a time that results in the unconstrained energy-optimal solution in the low-level problem. Furthermore, the effectiveness of the decentralized coordination framework at a corridor was validated in a field test in [30]. Rios-Torres and Malikopoulos [31] did a thorough literature review on the different methods of coordination of CAVs in their paper and discussed different remaining challenges and potential paths for future research. They classified coordination of CAVs in smart cities in two general groups, centralized and decentralized control. In centralized control, there is at least one task that is globally decided for CAVs in the system; however, in a decentralized approach, each CAV drives its optimal control input. In their survey, different approaches to coordination problem for CAVs were also mentioned such as reservation method [32–38], optimization travel time [39–47], multi-objective optimization [48–52], minimization of cars overlap in the intersection [53, 54], using queuing theory [55] and game theory approach [56]. In another survey, Guanetti et al. [57] discussed the state of the art on control and planning architecture for CAVs. They provided an overview of optimization-based approaches to CAVs control with the focus of improving energy efficiency.

The main objective of the approaches reported in the literature is to improve fuel efficiency and decrease traffic delays in the transportation network. Some approaches have considered a multi-objective problem to minimize both time and fuel consumption with different weights [58]. Other approaches have addressed the problem of coordinating CAVs at traffic scenarios involving a two-level joint optimization problem: (1) an upper-level vehicle coordination problem which specifies the sequence that each CAV crosses the intersection [59] and (2) a low-level optimal control problem in which each CAV derives its optimal acceleration/deceleration to cross the intersection.

Several research efforts have used scheduling theory for addressing the crossing intersection problem [60–65]. Colombo and Del Vecchio [62] proposed a least restrictive supervisor for intersection with collision avoidance constraints. Ahn et al. [60]

designed a supervisory controller by imposing a hard constraint on safety and studied its behavior in the presence of manual-driven cars. In a sequel paper, Ahn and Del Vecchio [63] introduced a supervisory controller for an intersection that overrides human-driven control input in case of a future accident. The authors used job-shop scheduling to solve the problem without considering the rear-end collision avoidance constraint. Guney and Raptis [65] proposed a centralized scheduling framework for coordination of CAVs crossing an intersection. In their approach, the intersection controller finds schedules, based on the rule of first-come-first-serve. Fayazi and Vahidi [64] considered a centralized intersection control server for CAVs crossing the intersection. The centralized intersection control server constantly solves an optimization problem for the coming CAVs and passes the optimal arrival time reducing the stop at the intersection and improving safety.

1.2.1 Control of CAVs under uncertainty

One restrictive assumption that has been made in most of the existing work is neglecting any source of uncertainty in the system. Due to the disturbances from the environment, noisy observations, and uncertainties in CAV's models, the deterministic framework for coordination of CAVs are prone to suboptimality and can even lead to unsafe conditions in real-world scenarios.

Xiao et al. [66] proposed a joint method of control barrier function and optimal control to improve the robustness in the presence of noise in coordinating CAV at merging roadways. Using the control barrier function, they tracked the prescribed optimal control trajectory in the presence of the uniformly distributed noise. Numerous other research efforts have been reported in the literature towards incorporating uncertainty in control of CAVs in scenarios such as overtaking, collision avoidance, adaptive cruise control (ACC), and cooperative adaptive cruise control (CACC).

Zhou et al. [67] proposed a receding horizon stochastic optimal control strategy for ACC and CACC to incorporate Gaussian noise in the system dynamics and

measurement. Using the separation principles, they decomposed the problem into two parts: 1) determining the feedback gains for the deterministic problem, and 2) estimating the system state by using the discrete Kalman filter. They employed dynamic programming with Lagrangian relaxation to solve the first problem. They also incorporated an adaptive Kalman filter to estimate the covariance matrix of system disturbances. Their proposed framework significantly outperformed the deterministic ACC and CACC when the system uncertainty was small, and measurement disturbances were large.

Vitus and Tomlin [68] presented a control framework for cooperation of CAVs in the presence of human-driven vehicles. They employed a chance-constrained formulation to avoid a traditional conservative solution resulting from considering the worst-case scenario for human-driven vehicles. They used sampling method to represent the system state and convex bounding method to handle the chance constraints. Gao et al. [69], proposed a control algorithm for an automated vehicle in overtaking of a human-driven vehicle based on its aggressiveness/ non-aggressiveness. They proposed (1) a robust algorithm with strict guarantees of collision-avoidance and (2) a stochastic algorithm with a small collision probability but possibly with shorter overtaking time. They demonstrated that for a non-aggressive human driver, the solution to the stochastic problem is less conservative. However, in the case of an aggressive human driver, both algorithms were equivalent.

In a survey paper, Carvalho et al. [70] classified various model predictive control (MPC) designs for intelligent vehicles under uncertainty into 1) tube-based Robust MPC, 2) linear time-varying Stochastic MPC, and 3) scenario-based MPC.
In a tube-based robust MPC approach, the notion of robust positively invariant (RPI) sets is used, in which if it is computed, robust constraint satisfaction can be guaranteed. However, the computation of the RPI set is generally difficult, and it can only be computed offline for linear systems. For the linear time-varying stochastic MPC approaches, finding analytical solutions are restricted to linear systems with normally

distributed additive disturbances. In scenario-based MPC, the intuition is to make the constraints of the MPC problem robustly safe in all of the scenarios. The benefits of sampling-based based MPC are flexibility in handling different types of uncertainties and easy implementation.

Liu et al. [71] presented linear-time-varying stochastic MPC to correct the driver's steering wherever there is a risk of unintended roadway departures. They used a probabilistic safety constraint that accounts for uncertainty in the driver's behavior. Carvalho et al. [72] proposed stochastic MPC for uncertain environment modeling. To formulate a chance-constrained MPC, they employed an Interacting Multiple Model Kalman Filter to predict positions of vehicles in the environment. Using constraint tightening and uncertainty propagation techniques, they solved the equivalent quadratic problem numerically.

Katriniok et al. [73] presented a scenario-based MPC, which prescribed speed advice to a human driver while considering an uncertain delay in their response to the advised speed trajectory. Their model provided a probabilistic guarantee on constraint satisfaction and collision avoidance. They validated their model through simulation and showed that it outperformed the baseline with neglecting uncertainty.

Another approach in online motion planning and decision making of CAVs is a sampling-based method. Dunlap et al. [74] proposed a sampling-based MPC for planning a safe path for an autonomous vehicle. Berntorp and Cairano [75] presented a probabilistic framework for online motion planning joint with decision making for CAVs using particle filtering. They integrated a nonlinear estimator with a sampling-based motion planner to compute candidate paths and corresponding state trajectories while accounting for an obstacle motion. They implemented the motion planner in receding horizon and validated it in the simulation. However, their focus was on online motion planning, rather than finding an optimal solution. Berntorp et al. [76] validated the proposed particle filtering strategy for online decision making and motion planning of CAVs on a small-scale robotics platform for several different scenarios, such as collision

avoidance, overtaking, and traffic-jam scenarios.

1.2.2 Research gaps

Most of the approaches reported in the literature to date refer to certain driving maneuvers such as overtaking (or driving) in the presence of human-driven vehicles. Using CAVs in real-world scenarios requires models that account for the uncertainty in the system, noise in the state observations, delays in the communication, and disturbances from the environment.

Several technical questions still remain unanswered. For example, what are the implications of the simplified models used to represent CAVs in the optimization and control analysis? Can we capture the real behavior of each CAV by introducing uncertainty in these models? Can we use simpler models to capture the vehicle dynamics and introduce the stochastic term to compensate for a potential mismatch? How can we model noise in the state observations in the optimization framework for CAVs? Can we guarantee safety with the existence of noisy observations or delays in the communication? How delays affect the performance of the coordination? How can we guarantee safety for CAVs if there are delays in the communication? Can we have robust coordination of CAVs if there is communication loss? How to maintain the stability of the system under those circumstances?

In this chapter, we completed the literature review and identified some major research gaps. In the next chapter, we present some preliminary work of CAV coordination, and then, in Chapter 3, we propose a research plan towards addressing the above gaps. Finally, we provide the expected contributions of this dissertation research with a provisional timeline in Chapter 4.

Chapter 2

PRELIMINARY RESULTS

In this chapter, we show some preliminary results on coordination of CAVs at different traffic scenarios, e.g., merging roadways, intersections, roundabouts, speed reduction zones, in the transportation system. In Section (2.1), we describe a problem of decentralized optimal control framework for CAVs at two interconnected intersections consists of two levels of control. In the upper-level control, we seek to minimize the travel time, and in the low-level problem, we find the optimal control policy for the constrained energy-minimization problem. We prove that rear-end safety constraint in this problem can only be activated instantly. Finally, we validate our hierarchical framework through simulation.

Next, in Section (2.2), we focus on the problem of coordination of the CAVs at a multi-lane roundabout. We validate an optimal control algorithm developed earlier in a multi-lane roundabout scenario using University of Delaware's scaled smart city (UDSSC). We first provide conditions where the solution is optimal. Then, we demonstrate the feasibility of the solution using experiments at UDSSC, and show that the optimal solution completely eliminates stop-and-go driving while preserving safety. Finally, we show the deviation from the planned trajectory, in the experimental testbed to motivate the importance of considering uncertainty in the motion control.

2.1 Hierarchical Optimal Coordination Framework for Connected and Automated Vehicles in Multiple Intersections

In this section, we present a decentralized optimal control framework for CAVs crossing two interconnected intersections. We develop a hierarchical optimization

framework that consists of upper-level and low-level problems. In the upper-level, we formulate a scheduling problem the solution of which designates the optimal time of each CAV to cross the intersections. The outcome of the upper-level scheduling problem becomes the input of the low-level problem. In particular, in the low-level, we formulate an optimal control problem the solution of which yields the optimal control input (acceleration/deceleration) of each CAV to exit the intersections at the time specified in the upper-level scheduling problem. We demonstrate the effectiveness of the proposed framework through simulation.

2.1.1 Problem Formulation

We consider two interconnected intersections shown in Fig. 2.1. A drone stores information about the geometric parameters of the intersections, the paths of the CAVs crossing the intersections, and schedules of CAVs. The intersections have a "control zone" (Fig. 2.1) inside of which the drone can communicate with the CAVs. The drone does not make any decision, and it only acts as a "coordinator" among the CAVs. We define the area where lateral collisions may occur as a "merging zone" (Fig. 2.1).

2.1.2 Modeling Framework

Let $N(t) \in \mathbb{N}$ be the number of CAVs inside the control zone at time $t \in \mathbb{R}^+$ and $\mathcal{N}(t) = \{1, \dots, N(t)\}$ be the queue that designates the order that each CAV enters the control zone. If two, or more, CAVs enter the control zone at the same time, the CAV with a shorter path receives a lower position in the queue; however, if the length of their path is the same, then their position is chosen arbitrarily. We partition the roads around the intersections into $n \in \mathbb{N}$ zones that belong to the set $\mathcal{M}$. Let $\mathcal{I}_i$ denotes the path of each CAV. When CAV $i \in \mathcal{N}(t)$ enters the control zone, it creates a tuple of the zones $\mathcal{I}_i := [m_1, \dots, m_n]$, $m_n \in \mathcal{M}$, $n \in \mathbb{N}$, that need to cross. Although the number n of partitions is arbitrary, choosing a big number increases the burden of computation for the scheduling problem, since CAV $i \in \mathcal{N}(t)$ needs to find its entry

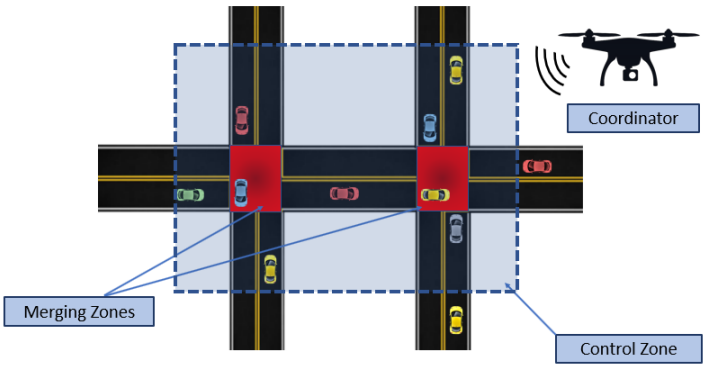

Figure 2.1: Two interconnected intersections with a drone as a coordinator.

time to each zone. We consider each road connecting to the merging zone to be a single zone. We also partition each merging zone into four smaller zones (Fig. 2.2). Without being restrictive in our analysis, the total number of zones in the intersections we consider here is $n = 22$.

Definition 2.1.1. *For each CAV $i \in \mathcal{N}(t)$, we define a tuple $\mathcal{C}_{i,j}$ of conflict zones with CAV $j \in \mathcal{N}(t)$, $j < i$,*

$$\mathcal{C}_{i,j} = [m \mid m \in \mathcal{M}, m \in \mathcal{I}_i \wedge m \in \mathcal{I}_j], \tag{2.1}$$

where the symbol "$\wedge$" corresponds to the logical "AND."

In Definition 1, the condition $j < i$ implies that CAV i only considers CAVs that are already within the control zone, i.e., their index in the queue is lower than i. Therefore, CAVs that are already inside the control zone do not need to address potential conflicts with a new CAV entering the control zone. For example in Fig. 2.2, CAV 3 has the following conflict tuples with CAV 1 and 2 respectively: $\mathcal{C}_{3,1} = [7]$ and $\mathcal{C}_{3,2} = [4, 13, 7, 8, 19]$.

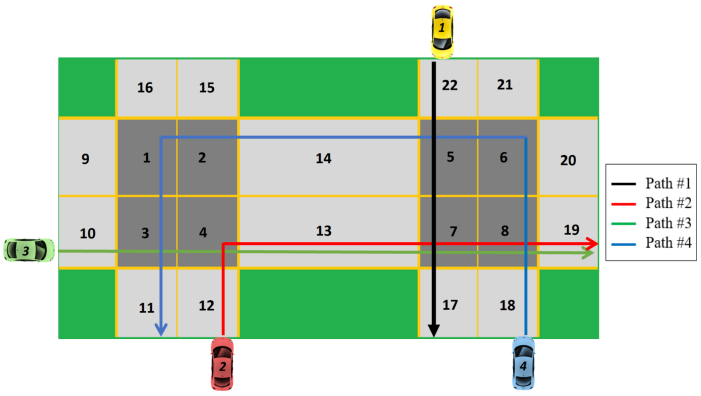

Figure 2.2: Zones numbered topologically and the fixed path for each CAV is shown.

2.1.3 CAV model and assumptions

We model the dynamic of each CAV $i \in \mathcal{N}(t)$ as a double integrator

$$\begin{aligned} \dot{p}_i(t) &= v_i(t), \\ \dot{v}_i(t) &= u_i(t), \end{aligned} \tag{2.2}$$

where $p_i(t) \in \mathcal{P}_i$, $v_i(t) \in \mathcal{V}_i$, and $u_i(t) \in \mathcal{U}_i$ denote position, speed and acceleration at $t \in \mathbb{R}^+$. Let $\boldsymbol{x}_i(t) = [p_i(t), v_i(t)]^T$, $u_i(t)$ be the state and control input of the CAV i at time t. Let t_i^0 and t_i^f be the time that CAV $i \in \mathcal{N}(t)$ enters and exits the control zone, and $\boldsymbol{x}_i^0 = [p_i(t_i^0), v_i(t_i^0)]^T$ be its initial state. For each CAV $i \in \mathcal{N}(t)$ control input and speed is bounded with the following constraints

$$u_{i,min} \leq u_i(t) \leq u_{i,max}, \tag{2.3}$$

$$0 < v_{\min} \leq v_i(t) \leq v_{\max}, \tag{2.4}$$

where $u_{i,min}, u_{i,max}$ are the minimum and maximum control inputs for each CAV $i \in \mathcal{N}(t)$ and $v_{\min}, v_{\max}$ are the minimum and maximum speed limit respectively. For simplicity, we do not consider diversity among CAVs. Thus, to this end, we set $u_{i,min} = u_{\min}$ and $u_{i,max} = u_{\max}$. The sets $\mathcal{P}_i$, $\mathcal{V}_i$ and $\mathcal{U}_i$, $i \in \mathcal{N}(t)$, are complete and totally bounded subsets of $\mathbb{R}$.

Definition 2.1.2. *Let CAV $k \in \mathcal{N}(t)$ be the preceding CAV of CAV $i \in \mathcal{N}(t)$ in zone $m \in \mathcal{M}$. The distance, $d^m(p_k(t), p_i(t))$, between i and k in zone m is*

$$d^m(p_k(t), p_i(t)) = (p_k(t) - d_k^{m,s}) - (p_i(t) - d_i^{m,s}), \tag{2.5}$$

where $d_i^{m,s}, d_k^{m,s} \in \mathbb{R}^+$ are the distance from the entry point of the control zone to the entry point of the conflict zone m for CAV i and k respectively.

To ensure the absence of rear-end collision between CAV $i \in \mathcal{N}(t)$ and the preceding CAV $k \in \mathcal{N}(t)$ in zone $m \in \mathcal{I}_i \wedge m \in \mathcal{I}_k$, we impose the following rear-end safety constraint

$$d^m(p_k(t), p_i(t)) \geq \delta_i(t), \tag{2.6}$$

where $\delta_i(t)$ is a predefined safe distance. The minimum safe distance $\delta_i(t)$ is a function of speed

$$\delta_i(t) = \gamma_i + \varphi v_i(t), \tag{2.7}$$

where γ_i is the standstill distance, and φ is the reaction time.

Assumption 2.1.3. *The path of each CAV is predefined, and all CAVs in the control zone have this information through the drone.*

Assumption 2.1.4. *There is no error or delay in any communication among the CAVs, and the CAVs to the drone.*

Assumption 2.1.5. *The speed at the boundaries of each zone is imposed and known.*

Assumption 2.1.6. *For CAV $i \in \mathcal{N}(t)$ the constraints (2.4) is not active at entrance of any zone $m \in \mathcal{I}_i$.*

The first assumption ensures that when a new CAV enters the control zone, it accesses the memory of the drone and discerns the path of CAVs that are inside the control zone. The second assumption may be strong, but it is relatively straightforward to relax it, as long as the noise or delays are bounded. The third assumption is used

to relax the constant speed assumption in the merging zone; see [77]. We can relax this assumption by estimating the speed at boundaries in the upper-level control for future. The fourth assumption is imposed based on the fact that CAVs would not violate any of the speed limits inside and outside the control zone. However, we can impose a *feasibility enforcement zone*, preceding the control zone, to ensure that the CAVs enter the control zone with the feasible speed; see [78].

2.1.4 Upper-level Problem: Scheduling

The objective of each CAV inside the control zone is to derive an optimal control input (acceleration/deceleration), which minimizes its travel time and energy consumption. The drone does not make any decision, and it only handles information among the CAVs. Each CAV derives its optimal control input in a two-level control framework. In the upper-level control, each CAV uses available information and solves the scheduling problem to compute the appropriate entry time to all zones along its path. Scheduling is a decision-making process that addresses the optimal allocation of resources to tasks over given time periods; see [79]. Thus, in what follows, we use the scheduling theory to find the time that CAV $i \in \mathcal{N}(t)$ has to reach the zone $m \in \mathcal{I}_i$. Each zone $m \in \mathcal{M}$ represents a "resource," and CAVs crossing this zone are the "jobs" assigned to the resource.

Definition 2.1.7. *The time that a CAV $i \in \mathcal{N}(t)$ enters each zone $m \in \mathcal{I}_i$ is called "schedule" and is denoted by $T_i^m \in \mathbb{R}^+$. For CAV $i \in \mathcal{N}(t)$, we define a "schedule tuple,"*

$$\mathcal{T}_i = [T_i^m \mid m \in \mathcal{I}_i]. \tag{2.8}$$

For example, the schedule tuple of CAV 1 in Fig. 2.2 is $\mathcal{T}^1 = [T_1^{22}, T_1^5, T_1^7, T_1^{17}]$. For each zone $m \in \mathcal{I}_i$, $i \in \mathcal{N}(t)$, the schedule $T_i^m \in \mathbb{R}^+$ is bounded by

$$T_i^{m-1} + R_i^{m-1} \leq T_i^m \leq T_i^{m-1} + D_i^{m-1}, \tag{2.9}$$

where $R_i^{m-1} \in \mathbb{R}^+$ is the shortest feasible time that it takes for CAV $i \in \mathcal{N}(t)$ to travel through the zone $m-1 \in \mathcal{I}_i$, while $D_i^{m-1} \in \mathbb{R}^+$ is the latest feasible time. Moreover, $R_i^{m-1} \in \mathbb{R}^+$ and $D_i^{m-1} \in \mathbb{R}^+$ are called the *release time* and the *deadline* of the job respectively. The schedule T_i^{m-1} is the time that CAV i enters the zone $m-1$, which is the zone before zone m. The exit time of CAV $i \in \mathcal{N}(t)$ from zone $m \in \mathcal{I}_i$ denoted by $T_i^{m'}$ and is equal to the entry time to zone $m+1 \in \mathcal{I}_i$; zone $m+1$ is the next zone that the CAV crosses right after zone m.

$$T_i^{m'} = T_i^{m+1}. \tag{2.10}$$

Definition 2.1.8. *For CAV $i \in \mathcal{N}(t)$ and $j \in \mathcal{N}(t)$, $j < i$ the safety constraint at the entry of zone $m \in \mathcal{C}_{i,j}$, with the minimum time gap $h \in \Gamma$, can be restated as*

$$|T_i^m - T_j^m| \geq h, \tag{2.11}$$

where Γ is set of all feasible time which do not activate (2.6) at the entry of zone m.

Remark 2.1.9. *Definition 2.1.8 relaxes the first-in-first-out (FIFO) entering policy to the conflict zone by restricting the absolute value of the difference between the two schedules.*

Problem 2.1.10. *For each CAV $i \in \mathcal{N}(t)$ with schedule tuple $\mathcal{T}_i$ and minimum time gap $h \in \mathbb{R}^+$, the scheduling problem is formulated as follows*

$$\begin{aligned} \min_{\mathcal{T}_i} \quad & J_i^{[1]}(\mathcal{T}_i) = t_i^f, \\ \text{subject to :} \quad & (2.9), (2.11). \end{aligned} \tag{2.12}$$

In our decentralized scheduling framework, upon entering the control zone, the CAVs solve the scheduling problem sequentially, based on their order at $\mathcal{N}(t)$. Then, they share their schedule tuples with the drone. For example for CAV 3 with $\mathcal{I}_3 =$

$[10, 3, 4, 13, 7, 8, 19]$, $\mathcal{C}_{3,1} = [7]$ and $\mathcal{C}_{3,2} = [4, 13, 7, 8, 19]$, we have the constraint (2.9) for each zone $m \in \mathcal{I}_3$ as

$$t_3^0 + R_3^{10} \leq T_3^3 \leq t_3^0 + D_3^{10}, \tag{2.13}$$

$$T_3^3 + R_3^3 \leq T_3^4 \leq T_3^3 + D_3^3, \tag{2.14}$$

$$T_3^4 + R_3^4 \leq T_3^{13} \leq T_3^4 + D_3^4, \tag{2.15}$$

$$T_3^{13} + R_3^{13} \leq T_3^7 \leq T_3^{13} + D_3^{13}, \tag{2.16}$$

$$T_3^7 + R_3^7 \leq T_3^8 \leq T_3^7 + D_3^7, \tag{2.17}$$

$$T_3^8 + R_3^8 \leq T_3^{19} \leq T_3^8 + D_3^8, \tag{2.18}$$

$$T_3^{19} + R_3^{19} \leq t_3^f \leq T_3^{19} + D_3^{19}, \tag{2.19}$$

and from the safety constraint (2.11) for $m \in \mathcal{C}_{3,1}$ and $m \in \mathcal{C}_{3,2}$ we have

$$|T_3^7 - T_1^7| \geq h, \tag{2.20}$$

$$|T_3^4 - T_2^4| \geq h, \tag{2.21}$$

$$|T_3^{13} - T_2^{13}| \geq h, \tag{2.22}$$

$$|T_3^7 - T_2^7| \geq h, \tag{2.23}$$

$$|T_3^8 - T_2^8| \geq h, \tag{2.24}$$

$$|T_3^{19} - T_2^{19}| \geq h, \tag{2.25}$$

where the schedule tuples of CAV 1 and 2 are accessible through the drone. CAV $i \in \mathcal{N}(t)$ needs to find the release time and the deadline of each zone $m \in \mathcal{I}_i$ prior to solving the scheduling problem (2.12).

Problem 2.1.11. *For each CAV $i \in \mathcal{N}(t)$ and each zone $m \in \mathcal{I}_i$, the release time R_i^m can be found by the following optimization problem*

$$\begin{aligned} \min_{u_i \in \mathcal{U}_i} \quad & J_i^{[2]}(u_i(t), t) = t_i^{e,m} - t_i^{s,m}, \\ \text{subject to:} \quad & (2.2), (2.3), (2.4), \\ \text{given} \quad & p_i(t_i^{s,m}), v_i(t_i^{s,m}), p_i(t_i^{e,m}), v_i(t_i^{e,m}), \end{aligned} \tag{2.26}$$

where $t_i^{s,m}$ and $t_i^{e,m}$ are the time that CAV $i \in \mathcal{N}(t)$ enters and exits the zone $m \in \mathcal{I}_i$ respectively. For zone $m \in \mathcal{I}_i$, evaluating the objective function at the optimal $u_i^*(t)$ results in the minimum time that CAV i can travel through zone m which is $R_i^m = t_i^{e,m} - t_i^{s,m}$.

By considering each CAV i to decelerate with $u_i(t) = u_{\min}$ and accelerate with $u_i(t) = u_{\max}$, each CAV $i \in \mathcal{N}(t)$ can find the deadline D_i^m and release time R_i^m for each zone $m \in \mathcal{I}_i$. If the deadline cannot satisfy either the boundary conditions or the speed constraint, then it decelerates with $u_i(t) = u_{\min}$ to reach $v_i(t) = v_{\min}$, cruises for some time, and then it accelerates with $u_i(t) = u_{\max}$. For example, consider CAV 3. After computing R_3^m and D_3^m for all $m \in \mathcal{I}_3$, it solves the scheduling Problem 2.1.10, the solution of which yields the schedule tuple $\mathcal{T}_3$.

2.1.5 Low-level problem: Energy Minimization

After addressing the scheduling in the upper-level problem, in the low-level problem, each CAV derives its minimum control input (acceleration/deceleration) that minimizes the energy consumption; see [80]. The problem is formulated as follows.

Problem 2.1.12. *For each CAV $i \in \mathcal{N}(t)$ and each zone $m \in \mathcal{I}_i$, the energy minimization problem is*

$$\begin{aligned} \min_{u_i \in \mathcal{U}_i} \quad & J_i^{[3]}(u_i(t), T_i^m, T_i^{m'}) = \tfrac{1}{2} \int_{T_i^m}^{T_i^{m'}} u_i(t)^2 dt, \\ \text{subject to:} \quad & (2.2), (2.3), (2.4), (2.6), \\ \text{given} \quad & p_i(T_i^m), v_i(T_i^m), p_i(T_i^{m'}), v_i(T_i^{m'}), T_i^m, T_i^{m'}, \end{aligned} \tag{2.27}$$

where T_i^m and $T_i^{m'}$ are the entry and exit time of CAV $i \in \mathcal{N}(t)$ from zone $m \in \mathcal{I}_i$.

2.1.6 Solution of low-level and upper-level problems

In the previous section, we described the hierarchical optimization framework that consists of two upper-level and one low-level problems. Upon entering the control zone, each CAV is added to the queue $\mathcal{N}(t)$,, and it solves the upper-level problems

(Problems 1 and 2) the solutions of which designate the optimal entry time to each zone along its path. In the upper-level problems, each CAV first derives the release time and deadline (Problem 2) prior to solving the scheduling problem (Problem 1). The outcome of the upper-level scheduling problem becomes the input of the low-level problem (Problem 3). In particular, in the low-level Problem 3, each CAV derives its optimal control input (acceleration/deceleration) that minimizes energy consumption along its path traveling at the time specified in the upper-level Problem 1. To this end, to simplify notation, we use p_i^s, v_i^s, p_i^e and v_i^e instead of $p_i(t_i^{s,m})$, $v_i(t_i^{s,m})$, $p_i(t_i^{e,m})$ and $v_i(t_i^{e,m})$ respectively.

2.1.7 Analytical solution of the release time and the deadline

For the analytical solution of the release time problem (Problem 2.1.11), we apply Hamiltonian analysis. For each CAV $i \in \mathcal{N}(t)$ the Hamiltonian function with the state and control constraints adjoined is

$$\begin{aligned} H_i(t, p_i(t), v_i(t), u_i(t)) &= 1 + \lambda_i^p v_i(t) + \lambda_i^v u_i(t) \\ &+\mu_i^a(u_i(t) - u_{\max}) + \mu_i^b(u_{\min} - u_i(t)) \\ &+\mu_i^c(v_i(t) - v_{\max}) + \mu_i^d(v_{\min} - v_i(t)), \end{aligned} \tag{2.28}$$

where λ_i^p and λ_i^v are costates, and μ^T is a vector of a lagrange multipliers:

$$\mu_i^a = \begin{cases} > 0 & u_i(t) - u_{\max} = 0 \\ = 0 & u_i(t) - u_{\max} < 0 \end{cases}, \tag{2.29}$$

$$\mu_i^b = \begin{cases} > 0 & u_{\min} - u_i(t) = 0 \\ = 0 & u_{\min} - u_i(t) < 0 \end{cases}, \tag{2.30}$$

$$\mu_i^c = \begin{cases} > 0 & v_i(t) - v_{\max} = 0 \\ = 0 & v_i(t) - v_{\max} < 0 \end{cases}, \tag{2.31}$$

$$\mu_i^d = \begin{cases} > 0 & v_{\min} - v_i(t) = 0 \\ = 0 & v_{\min} - v_i(t) < 0 \end{cases}. \tag{2.32}$$

The Euler-Lagrange equations become:

$$\dot{\lambda_i^p} = -\frac{\partial H_i}{\partial p_i} = 0, \tag{2.33}$$

$$\dot{\lambda_i^v} = -\frac{\partial H_i}{\partial v_i} = -\lambda_i^p - \mu_i^c + \mu_i^d. \tag{2.34}$$

2.1.7.1 State constraints are not active

First, we consider the case where the state constraint (2.4) does not become active, hence $\mu_i^c = \mu_i^d = 0$.

Lemma 2.1.13. *The optimal control input of the release time problem (Problem 2.1.11), without the state constraint, switches at most once, and it can be equal to either* $u_{\min}$*,* *or* $u_{\max}$*,* *or* $u_{\max}$ *then* $u_{\min}$*.*

Proof. If the state constraints for the release time problem (Problem 2.1.11) are not active, then $\mu_j^c = \mu_j^d = 0$. Solving (2.33) and (2.34) simultaneously yields $\lambda_i^p(t) = a_i$ and $\lambda_i^v(t) = -a_i t + b_i$, where a_i, b_i are the constants of integration. Hence

$$u_i(t) = \begin{cases} u_{\min}, & \text{if} \quad \lambda_i^v(t) > 0 \\ u_{\max}, & \text{if} \quad \lambda_i^v(t) < 0 \end{cases}. \tag{2.35}$$

It follows immediately from the linearity of $\lambda_i^v(t)$ that its sign can change at most once. For the second statement, we use the fact that we can have at most one switching point. There are four cases that we should consider: Case 1: $u_{\min}$, Case 2: $u_{\max}$, Case 3: $u_{\max}$ then $u_{\min}$, and Case 4: $u_{\min}$ then $u_{\max}$. The initial and final states, denoted by $[p_i^s, v_i^s]^T$ and $[p_i^e, v_i^e]^T$ respectively, are known.

Case 1: If CAV $i \in \mathcal{N}(t)$ decelerates with $u_{\min}$, then from (2.2) its final speed is

$$v_i^f = \sqrt{2u_{\min} \cdot (p_i^e - p_i^s) + v_i^{s2}}. \tag{2.36}$$

This case is feasible.

Case 2: If CAV $i \in \mathcal{N}(t)$ accelerates with $u_{\max}$, similarly from (2.2) its final speed is

$$v_i^f = \sqrt{2u_{\max} \cdot (p_i^e - p_i^s) + v_i^{s2}}. \tag{2.37}$$

This case is feasible.

Case 3: We have $u_{\max}$ then $u_{\min}$, this implies the following:

$$\lambda_i^v(t) = \begin{cases} - & \text{, if} \quad t_i^{s,m} \leq t < t_i^{c,m} \\ 0 & \text{, if} \quad t = t_i^{c,m} \\ + & \text{, if} \quad t_i^{c,m} < t \leq t_i^{e,m} \end{cases}, \tag{2.38}$$

where $\dot{\lambda_i^v}(t) = -\lambda_i^p(t) = -a_i > 0$. Evaluating the Hamiltonian along the optimal control at time $t_i^{c,m}$ yields

$$H_i(t_i^{c,m}, p_i(t_i^{c,m}), v_i(t_i^{c,m}), u_i(t_i^{c,m})) = 1 + \lambda_i^p v_i(t_i^{c,m}). \tag{2.39}$$

From the transversality condition,

$$H_i(t_i^{e,m}, p_i(t_i^{e,m}), v_i(t_i^{e,m}), u_i(t_i^{e,m})) = 0. \tag{2.40}$$

The Hamiltonian (2.28) must be constant along the optimal solution, since it is not an explicit function of time

$$1 + \lambda_i^p v_i(t_i^{c,m}) = 0. \tag{2.41}$$

Hence, $v_i(t_i^{c,m}) = -\frac{1}{\lambda_i^p} > 0$. As long as the initial point and endpoint conditions are satisfied, this case is feasible.

Case 4 : Similarly to Case 3, it can be shown that $\lambda_i^p(t) = a_i > 0$. Solving (2.41) for $v_i(t_i^{c,m})$, we have $v_i(t_i^{c,m}) = -\frac{1}{\lambda_i^p} < 0$. Hence, this case cannot be a feasible solution. □

Lemma 2.1.14. *Let $x_i^0 = [p_i^s, v_i^s]^T$ and $x_i^e = [p_i^e, v_i^e]^T$ be the initial and final states of CAV $i \in \mathcal{N}(t)$ travelling in zone $m \in \mathcal{I}_i$. Let $x_i^c = [p_i^c, v_i^c]^T$ be the intermediate state at the switching point. Then,*

$$p_i^c = \frac{v_i^{e2} - v_i^{s2} + 2(u_{\max} p_i^s - u_{\min} p_i^e)}{2(u_{\max} - u_{\min})}, \tag{2.42}$$

$$v_i^c = \sqrt{v_i^{s2} + 2u_{\max} \cdot (p_i^c - p_i^s)}. \tag{2.43}$$

Proof. From (2.2) and Lemma 2.1.13, the intermediate states is found by solving the following system of equations

$$\begin{cases} v_i^{c2} - v_i^{s2} = 2u_{\max} \cdot (p_i^c - p_i^s) \\ v_i^{e2} - v_i^{c2} = 2u_{\min} \cdot (p_i^e - p_i^c) \end{cases}, \tag{2.44}$$

which yields (2.42) and (2.43). □

Proposition 2.1.15. *The release time of CAV $i \in \mathcal{N}(t)$ travelling in zone $m \in \mathcal{I}_i$ for the unconstrained case is*

$$R_i^m = \frac{v_i^c - v_i^s}{u_{\max}} + \frac{v_i^e - v_i^c}{u_{\min}}. \tag{2.45}$$

Proof. The total time is found by integrating (2.2) for $u_i = u_{\max}$ and $u_i = u_{\min}$.

$$\begin{aligned} v_i^c - v_i^s &= u_{\max} \cdot (t_i^{c,m} - t_i^{s,m}), \quad \forall\, t \in [t_i^{s,m}, t_i^{c,m}], \\ v_i^e - v_i^c &= u_{\min} \cdot (t_i^{e,m} - t_i^{c,m}), \quad \forall\, t \in [t_i^{c,m}, t_i^{e,m}]. \end{aligned} \tag{2.46}$$

Solving (2.46) for $t_i^{c,m}$ and $t_i^{e,m}$, the result follows

$$t_i^{c,m} = \frac{v_i^c - v_i^s}{u_{\max}} + t_i^{s,m}, \tag{2.47}$$

$$t_i^{e,m} = \frac{v_i^c - v_i^s}{u_{\max}} + \frac{v_i^e - v_i^c}{u_{\min}} + t_i^{s,m}. \tag{2.48}$$

Substituting $t_i^{e,m}$ into $R_i^m = t_i^{e,m} - t_i^{s,m}$ we have (2.45). □

Proposition 2.1.16. *Let $x_i^0 = [p_i^s, v_i^s]^T$ and $x_i^e = [p_i^e, v_i^e]^T$ be the initial and final states of CAV $i \in \mathcal{N}(t)$ and $x_i^c = [p_i^c, v_i^c]^T$ be the intermediate state at the switching point. The deadline of CAV i travelling in zone $m \in \mathcal{I}_i$ for the unconstrained case is*

$$D_i^m = \frac{v_i^c - v_i^s}{u_{\min}} + \frac{v_i^e - v_i^c}{u_{\max}}, \tag{2.49}$$

$$v_i^c = \sqrt{v_i^{s2} + 2u_{\min} \cdot (p_i^c - p_i^s)}, \tag{2.50}$$

$$p_i^c = \frac{v_i^{e2} - v_i^{s2} + 2(u_{\min} p_i^s - u_{\max} p_i^e)}{2(u_{\max} - u_{\min})}. \tag{2.51}$$

Proof. The control input of CAV $i \in \mathcal{N}(t)$ in zone $m \in \mathcal{I}_i$ consists of two arcs, decelerating with $u_i(t) = u_{\min}$ and accelerating with $u_i(t) = u_{\max}$. Similarly to the Lemma 2.1.14, (2.51) and (2.50) are found. The total time for each arc is found by integrating (2.2)

$$\begin{aligned} v_i^c - v_i^s &= u_{\min} \cdot (t_i^{c,m} - t_i^{s,m}), \quad \forall\, t \in [t_i^{s,m}, t_i^{c,m}], \\ v_i^e - v_i^c &= u_{\max} \cdot (t_i^{e,m} - t_i^{c,m}), \quad \forall\, t \in [t_i^{c,m}, t_i^{e,m}]. \end{aligned} \tag{2.52}$$

Solving (2.52) for $t_i^{c,m}$ and $t_i^{e,m}$, we have

$$t_i^{c,m} = \frac{v_i^c - v_i^s}{u_{\min}} + t_i^{s,m}, \tag{2.53}$$

$$t_i^{e,m} = \frac{v_i^c - v_i^s}{u_{\min}} + \frac{v_i^e - v_i^c}{u_{\max}} + t_i^{s,m}. \tag{2.54}$$

Substituting $t_i^{e,m}$ into $D_i^m = t_i^{e,m} - t_i^{s,m}$ we have (2.49). □

Remark 2.1.17. *CAV $i \in \mathcal{N}(t)$, travelling in zone $m \in \mathcal{I}_i$ with $D_i^m = t_i^{e,m} - t_i^{s,m}$, activates the state constraint $v_i(t) = v_{\min}$, if the speed at the intermediate point derived by (2.50) is either imaginary, or violates the speed constraint (2.4).*

2.1.7.2 State constraints are active

Next, We consider the cases where the speed constraints become active.

Theorem 2.1.18. *In Problem 2.1.11, if there is no switching point of the control input, then none of the speed constraints become active.*

Proof. We consider the two cases that there is no switching point i.e., Case 1: $u_{\min}$, Case 2: $u_{\max}$.

Case 1: For all $t < t' \in [t_i^{s,m}, t_i^{e,m}]$, we have

$$v_i(t) > v_i(t'), \tag{2.55}$$

Hence, the minimum and maximum speed can only occur at $t_i^{e,m}$ and $t_i^{s,m}$ respectively, namely

$$v_i^e \leq v_i(t), \quad \forall\, t \in [t_i^{s,m}, t_i^{e,m}], \tag{2.56}$$

and

$$v_i(t) \leq v_i^s, \quad \forall\, t \in [t_i^{s,m}, t_i^{e,m}]. \tag{2.57}$$

However, from Assumption 2.1.6,

$$v_{\min} < v_i^e \leq v_i(t) \leq v_i^s < v_{\max}, \quad \forall\, t \in [t_i^{s,m}, t_i^{e,m}]. \tag{2.58}$$

Case 2: Similarly to Case 1, we have

$$v_{\min} < v_i^s \leq v_i(t) \leq v_i^e < v_{\max}, \quad \forall\, t \in [t_i^{s,m}, t_i^{e,m}]. \tag{2.59}$$

□

Corollary 2.1.19. *For CAV $i \in \mathcal{N}(t)$ in zone $m \in \mathcal{I}_i$, the unconstrained solution of the release time problem (Problem 2.1.11) can not lead into activating the constrained arc $v_i(t) = v_{\min}$.*

Proof. From Theorem 2.1.18, we know in case of no switching point none of the speed constraints become active. Now we consider having one switching point at time $t_i^{c,m} \in [t_i^{s,m}, t_i^{e,m}]$, we have

$$u_i(t) = u_{\max} > 0 \tag{2.60}$$

$$v_i^s \leq v_i(t), \quad \forall\, t \in [t_i^{s,m}, t_i^{c,m}], \tag{2.61}$$

$$u_i(t) = u_{\min} < 0 \tag{2.62}$$

$$v_i^e \leq v_i(t), \quad \forall\ t \in [t_i^{c,m}, t_i^{e,m}], \tag{2.63}$$

Therefore, it follows that the minimum speed of CAV i for all $t \in [t_i^{s,m}, t_i^{e,m}]$ is either v_i^e or v_i^s. From Assumption 2.1.6, state constraints are not active at the entry and exit of the zones, and the proof is complete. □

One can check whether the unconstrained solution of CAV i leads to violation of the speed constraint $v_i(t) \leq v_{\max}$ in zone m, by checking the speed at the interior point v_i^c found from (2.43). If the unconstrained solution violates the speed constraint $v_i(t) \leq v_{\max}$, then the solution exits the unconstrained arc at time τ_1, and enters the constrained arc $v_i(t) = v_{\max}$. Then the unconstrained arc is pieced together with the constrained arc $v_i(t) = v_{\max}$, and we re-solve the problem with the two arcs pieced together. The two arcs yield a set of algebraic equations that are solved simultaneously using the boundary conditions and interior conditions between the arcs. From Assumption 2.1.6, the speed at the boundary of zones do not activate the speed constraint; therefore, the solution can not stay at the constrained arc $v_i(t) = v_{\max}$ and it must exit the constrained arc $v_i(t) = v_{\max}$ at time τ_2. The unconstrained and constrained arcs are pieced together, and we re-solve the problem with the three arcs pieced together.

Theorem 2.1.20. *The release time of CAV $i \in \mathcal{N}(t)$ travelling in zone $m \in \mathcal{I}_i$ for the constrained case $v_i(t) = v_{\max}$ is*

$$R_i^m = \frac{a_i + b_i}{2u_{\min}\ u_{\max}\ v_{\max}}, \tag{2.64}$$

where

$$a_i = v_i^{s2}\ u_{\min} - v_i^{e2}\ u_{\max} + (u_{\min} - u_{\max})\ v_{\max}^2, \tag{2.65}$$

$$b_i = 2u_{\min}\ u_{\max}(p_i^e - p_i^s) + 2v_{\max}\ (v_i^e\ u_{\max} - v_i^s\ u_{\min}). \tag{2.66}$$

Proof. Let CAV $i \in \mathcal{N}(t)$ enter and exit the zone $m \in \mathcal{I}_i$ at t_i^s and t_i^e respectively. From the boundary conditions, we have $p_i(t_i^s) = p_i^s$, $v_i(t_i^s) = v_i^s$, $p_i(t_i^e) = p_i^e$ and $v_i(t_i^e) = v_i^e$.

CAV i cruises with $u_i(t) = u_{\max}$, and then it enters the constrained arc $v_i(t) = v_{\max}$ at time τ_1. It stays at the constrained arc with $u_i(t) = 0$ until time τ_2. After exiting the constrained arc, it decelerates with $u_i(t) = u_{\min}$. Substituting optimal control input in (2.2) results to the following optimal state equations.

$$\begin{aligned} p_i^*(t) =& \frac{1}{2}u_{\max}(t^2 - t_i^{s2}) - u_{\max}t_i^s(t - t_i^s) + v_i^s(t - t_i^s) + p_i^s, \\ v_i^*(t) =& u_{\max}(t - t_i^s) + v_i^s, \quad \forall\, t \in [t_i^s, \tau_1^-]. \end{aligned} \tag{2.67}$$

$$\begin{aligned} p_i^*(t) =& v_{\max}(t - \tau_1) + p_i^*(\tau_1^+), \\ v_i^*(t) =& v_{\max}, \quad \forall\, t \in [\tau_1^+, \tau_2^-]. \end{aligned} \tag{2.68}$$

$$\begin{aligned} p_i^*(t) =& \frac{1}{2}u_{\min}(t^2 - \tau_2^2) - u_{\min}\tau_2(t - \tau_2) \\ &+ v_i^*(\tau_2^+)(t - \tau_2) + p_i^*(\tau_2^+), \\ v_i^*(t) =& u_{\min}(t - \tau_2) + v_i^*(\tau_2^+), \quad \forall\, t \in [\tau_2^+, t_i^e]. \end{aligned} \tag{2.69}$$

The states of CAV are continuous at τ_1 and τ_2, thus

$$p_i^*(\tau_1^-) = p_i^*(\tau_1^+) \tag{2.70}$$

$$v_i^*(\tau_1^-) = v_i^*(\tau_1^+), \tag{2.71}$$

$$p_i^*(\tau_2^-) = p_i^*(\tau_2^+), \tag{2.72}$$

$$v_i^*(\tau_2^-) = v_i^*(\tau_2^+). \tag{2.73}$$

From (2.70)-(2.73) and the boundary conditions, piecing the unconstrained and constrained arcs together, we have

$$\begin{aligned} p_i^*(\tau_1) =& \frac{1}{2}u_{\max}(\tau_1^2 - t_i^s) - u_{\max}t_i^s(\tau_1 - t_i^s) \\ &+ v_i^s(\tau_1 - t_i^s) + p_i^s, \end{aligned} \tag{2.74}$$

$$\tau_1 = \frac{v_{\max} - v_i^s}{u_{\max}} + t_i^s, \tag{2.75}$$

$$p_i^*(\tau_2) = v_{\max}(\tau_2 - \tau_1) + p_i^*(\tau_1), \tag{2.76}$$

$$v_i^*(\tau_2) = v_{\max}, \tag{2.77}$$

$$p_i^e = \frac{1}{2}u_{\min}(t_i^{e2} - \tau_2^2) - u_{\min}\tau_2(t_i^e - \tau_2) + v_i^*(\tau_2)(t_i^e - \tau_2) + p_i^*(\tau_2), \tag{2.78}$$

$$v_i^e = u_{\min}(t_i^e - \tau_2) + v_i^*(\tau_2). \tag{2.79}$$

Solving the system of equations above results to (2.64). □

Proposition 2.1.21. *Let τ_1 and τ_2 be the time that CAV $i \in \mathcal{N}(t)$ travels in the constrained arc $v_i(t) = v_{\min}$, while it is in zone $m \in \mathcal{I}_i$. Let $[p_i^s, v_i^s]^T$ and $[p_i^e, v_i^e]^T$ be the initial and final states of CAV i in zone m respectively. The deadline of CAV i for zone m is computed as follows*

$$D_i^m = \frac{v_i^e - v_{\min}}{u_{\max}} + \tau_2 - t_i^{s,m}, \tag{2.80}$$

where

$$\tau_2 = \frac{p_i(\tau_2) - p_i(\tau_1)}{v_{\min}} + \tau_1, \tag{2.81}$$

$$p_i(\tau_2) = \frac{v_{\min}^2 - v_i^{e2}}{2\ u_{\max}} + p_i^e, \tag{2.82}$$

$$p_i(\tau_1) = \frac{v_{\min}^2 - v_i^{s2}}{2\ u_{\min}} + p_i^s, \tag{2.83}$$

$$\tau_1 = \frac{-v_i^s + v_{\min}}{u_{\min}} + t_i^{s,m}. \tag{2.84}$$

Proof. Let CAV $i \in \mathcal{N}(t)$ enter and exit the zone $m \in \mathcal{I}_i$ at t_i^s and t_i^e respectively. From the boundary conditions, we have $p_i(t_i^s) = p_i^s$, $v_i(t_i^s) = v_i^s$, $p_i(t_i^e) = p_i^e$ and $v_i(t_i^e) = v_i^e$. CAV i decelerates with $u_i(t) = u_{\min}$ then it enters the constrained arc $v_i(t) = v_{\min}$ at time τ_1. It stays at constrained arc with $u_i(t) = 0$ until the τ_2. After exiting the

constrained arc, it cruises with $u_i(t) = u_{\max}$. Substituting optimal control input in (2.2) results to the following optimal state equations.

$$\begin{aligned} p_i^*(t) =& \frac{1}{2}u_{\min}(t^2 - t_i^{s2}) - u_{\min}t_i^s(t - t_i^s) + v_i^s(t - t_i^s) + p_i^s, \\ v_i^*(t) =& u_{\min}(t - t_i^s) + v_i^s, \quad \forall\, t \in [t_i^s, \tau_1^-]. \end{aligned} \tag{2.85}$$

$$\begin{aligned} p_i^*(t) =& v_{\min}(t - \tau_1) + p_i^*(\tau_1^+), \\ v_i^*(t) =& v_{\min}, \quad \forall\, t \in [\tau_1^+, \tau_2^-]. \end{aligned} \tag{2.86}$$

$$\begin{aligned} p_i^*(t) =& \frac{1}{2}u_{\max}(t^2 - \tau_2^2) - u_{\max}\tau_2(t - \tau_2) \\ & + v_i^*(\tau_2^+)(t - \tau_2) + p_i^*(\tau_2^+), \\ v_i^*(t) =& u_{\max}(t - \tau_2) + v_i^*(\tau_2^+), \quad \forall\, t \in [\tau_2^+, t_i^e]. \end{aligned} \tag{2.87}$$

The states of CAV are continuous at τ_1 and τ_2, thus

$$p_i^*(\tau_1^-) = p_i^*(\tau_1^+), \tag{2.88}$$

$$v_i^*(\tau_1^-) = v_i^*(\tau_1^+), \tag{2.89}$$

$$p_i^*(\tau_2^-) = p_i^*(\tau_2^+), \tag{2.90}$$

$$v_i^*(\tau_2^-) = v_i^*(\tau_2^+). \tag{2.91}$$

From (2.88)-(2.91) and the boundary conditions, piecing the unconstrained and constrained arcs together, we have

$$\begin{aligned} p_i^*(\tau_1) = & \frac{1}{2}u_{\min}(\tau_1^2 - t_i^s) - u_{\min}t_i^s(\tau_1 - t_i^s) \\ & + v_i^s(\tau_1 - t_i^s) + p_i^s, \end{aligned} \tag{2.92}$$

$$\tau_1 = \frac{v_{\min} - v_i^s}{u_{\min}} + t_i^s, \tag{2.93}$$

$$p_i^*(\tau_2) = v_{\min}(\tau_2 - \tau_1) + p_i^*(\tau_1), \tag{2.94}$$

$$v_i^*(\tau_2) = v_{\min}, \tag{2.95}$$

$$\begin{aligned} p_i^e = & \frac{1}{2}u_{\max}(t_i^{e2} - \tau_2^2) - u_{\max}\tau_2(t_i^e - \tau_2), \\ & + v_i^*(\tau_2)(t_i^e - \tau_2) + p_i^*(\tau_2), \end{aligned} \tag{2.96}$$

$$v_i^e = u_{\max}(t_i^e - \tau_2) + v_i^*(\tau_2). \tag{2.97}$$

Solving the system of equations above results to (2.80). □

2.1.8 Solution of the scheduling problem (Problem 2.1.10)

In the scheduling problem (Problem 2.1.10), the safety constraint (2.11) is a disjunctive constraint that

$$T_i^m - T_j^m \geq h, \tag{2.98}$$

or

$$-(T_i^m - T_j^m) \geq h. \tag{2.99}$$

In disjunctive constraints, only one constraint has to be satisfied. By introducing a binary variable $B_i \in \{0, 1\}$ and big number $M \in \mathbb{R}^+$, we rewrite the disjunctive constraints as two separate constraints as following:

$$(T_i^m - T_j^m) + B_i \cdot M \geq h, \tag{2.100}$$

or

$$-(T_i^m - T_j^m) + (1 - B_i) \cdot M \geq h. \tag{2.101}$$

After transforming the safety constraint to two separate constraints, we use a mixed-integer linear program to solve the scheduling problem. Upon entering the control zone, CAV $i \in \mathcal{N}(t)$ solves the scheduling problem, which results in schedule tuple $\mathcal{T}_i$.

2.1.9 Analytical solution of the energy minimization problem (Problem 2.1.12)

One approach to address the inequality constraints, which are a function of state variables, is adjoining the qth-order state variable inequality constraint to the Hamiltonian function. The qth-order state variable inequality constraint can be found by taking the successive total time derivative of constraint and substitute (2.2) for $\dot{\mathbf{x}}$ until we obtain an expression that is explicitly dependent on the control variable;

see [81]. For each CAV $i \in \mathcal{N}(t)$, with CAV $k \in \mathcal{N}(t)$ positioned immediately in front of it, the Hamiltonian is

$$\begin{aligned} H_i(t, p_i(t), v_i(t), u_i(t)) &= \frac{1}{2}u_i(t)^2 + \lambda_i^p v_i(t) + \lambda_i^v u_i(t) \\ &+\mu_i^a(u_i(t) - u_{\max}) + \mu_i^b(u_{\min} - u_i(t)) \\ &+\mu_i^c(u_i(t)) + \mu_i^d(-u_i(t)) \\ &+\mu_i^s(v_i(t) - v_k(t) + \varphi u_i(t)). \end{aligned} \tag{2.102}$$

where λ_i^p and λ_i^v are costates, and μ^T is a vector of a lagrange multipliers.

2.1.9.1 State and control constraints are not active

If the state and control constraints are not active, $\mu_i^a = \mu_i^b = \mu_i^c = \mu_i^d = 0$ and the solution; see [24], is

$$u_i^* = a_i t + b_i, \tag{2.103}$$

by substituting (2.103) in (2.2) we have

$$v_i^* = \frac{1}{2}a_i t^2 + b_i t + c_i, \tag{2.104}$$

$$p_i^* = \frac{1}{6}a_i t^3 + \frac{1}{2}b_i t^2 + c_i t + d_i. \tag{2.105}$$

In the above equations a_i, b_i, c_i, d_i are constants of integration, which are found by substituting the initial and final states $p_i(T_i^m), v_i(T_i^m)$, $p_i(T_i^{m'})$ and $v_i(T_i^{m'})$ in zone $m \in \mathcal{I}_i$. Thus, a system of equations in the form of $\mathbf{T}_i\mathbf{b}_i = \mathbf{q}_i$, is

$$\begin{bmatrix} \frac{1}{6}(T_i^m)^3 & \frac{1}{2}(T_i^m)^2 & (T_i^m) & 1 \\ \frac{1}{2}(T_i^m)^2 & (T_i^m) & 1 & 0 \\ \frac{1}{6}(T_i^{m'})^3 & \frac{1}{2}(T_i^{m'})^2 & (T_i^{m'}) & 1 \\ \frac{1}{2}(T_i^{m'})^2 & (T_i^{m'}) & 1 & 0 \end{bmatrix} \cdot \begin{bmatrix} a_i \\ b_i \\ c_i \\ d_i \end{bmatrix} = \begin{bmatrix} p_i(T_i^m) \\ v_i(T_i^m) \\ p_i(T_i^{m'}) \\ v_i(T_i^{m'}) \end{bmatrix}. \tag{2.106}$$

Note that since (2.106) can be computed online, the controller may re-evaluate the four constants at any time $t \in [T_i^m, T_i^{m'}]$ and update (2.103).

There are different cases that can happen and activate either the state or control constraints. Next, we consider the cases that CAV only travels on the constrained arcs except the rear-end safety (2.6).

2.1.9.2 CAV travels on different constrained arcs

Case 1: CAV $i \in \mathcal{N}(t)$ enters the constrained arc $u_i(t) = u_{\max}$ at T_i^m. Then, it moves to the constrained arc $u_i(t) = u_{\min}$ at τ_1 and stays on it until T_i^{m+1}.

Theorem 2.1.22. *Let T_i^m and T_i^{m+1} be the schedules of CAV $i \in \mathcal{N}(t)$ for zones $m, m+1 \in \mathcal{I}_i$ respectively, where zone $m+1$ follows m. In zone m, the CAV i first travels in the constrained arc $u_i(t) = u_{\max}$ and then in the constrained arc $u_i(t) = u_{\min}$, if the speed constraint does not become active in zone m and*

$$T_i^{m+1} - T_i^m = R_i^m. \tag{2.107}$$

Proof. Let CAV $i \in \mathcal{N}(t)$ enter and and exit the zone $m \in \mathcal{I}_i$ at T_i^m and $T_i^{m'}$ respectively. Substituting (2.10) into $T_i^{m+1} - T_i^m = R_i^m$, we have $T_i^{m'} - T_i^m = R_i^m$. Thus, CAV i is traveling at the earliest feasible time in zone m. Since the speed constraint is not active, the solution is equivalent to the solution of the release time problem (Problem 2.1.11) when the speed constraint is not active. □

In the above case, the optimal control input is

$$u_i^*(t) = \begin{cases} u_{\max} & \text{, if} \quad T_i^m \le t < \tau_1 \\ u_{\min} & \text{, if} \quad \tau_1 \le t \le T_i^{m'} \end{cases}. \tag{2.108}$$

Substituting (2.108) in (2.2), we have

$$\begin{aligned} p_i^*(t) =& \frac{1}{2} u_{\max} t^2 + b_i t + c_i, \\ v_i^*(t) =& u_{\max} t + b_i, \qquad\qquad \forall\ t \in [T_i^m, \tau_1^-], \end{aligned} \tag{2.109}$$

$$
\begin{aligned}
p_i^*(t) =& \frac{1}{2}u_{\min}t^2 + d_i t + e_i, \\
v_i^*(t) =& u_{\min}t + d_i, \qquad\qquad \forall\ t \in [\tau_1^+, T_i^{m'}],
\end{aligned} \tag{2.110}
$$

where b_i, c_i, d_i and e_i are constants of integration, which are found by using initial conditions $p_i(T_i^m), v_i(T_i^m)$ and final conditions $p_i(T_i^{m'}), v_i(T_i^{m'})$ of the CAV in zone $m \in \mathcal{I}_i$. The switching point τ_1 can be found from (2.47).

Case 2: CAV i enters the constrained arc $u_i(t) = u_{\max}$ at T_i^m, then it moves to the constrained arc $v_i(t) = v_{\max}$ at $t = \tau_1$. It exits the constrained arc $v_i(t) = v_{\max}$ at $t = \tau_2$, and it enters the constrained arc $u_i(t) = u_{\min}$ and stays on it until T_i^{m+1}.

Corollary 2.1.23. *CAV $i \in \mathcal{N}(t)$ travels in zone $m \in \mathcal{I}_i$ similarly to Case 2, if the speed constraint becomes active in zone m and (2.107) holds.*

Proof. As in Theorem (2.1.22), the solution is equivalent to the solution of the release time problem (Problem 2.1.11) when the speed constraint is active. □

In the above case, the optimal control input is

$$
u_i^*(t) = \begin{cases} u_{\max} & \text{, if} \quad T_i^m \le t < \tau_1 \\ 0 & \text{, if} \quad \tau_1 \le t \le \tau_2 \\ u_{\min} & \text{, if} \quad \tau_2 \le t \le T_i^{m'} \end{cases}. \tag{2.111}
$$

Substituting (2.111) in (2.2), we have

$$
\begin{aligned}
p_i^*(t) =& \frac{1}{2}u_{\max}t^2 + b_i t + c_i, \\
v_i^*(t) =& u_{\max}t + b_i, \qquad\qquad \forall\ t \in [T_i^m, \tau_1^-],
\end{aligned} \tag{2.112}
$$

$$
\begin{aligned}
p_i^*(t) =& v_{\max}t + d_i, \\
v_i^*(t) =& v_{\max}, \qquad\qquad \forall\ t \in [\tau_1^+, \tau_2^-],
\end{aligned} \tag{2.113}
$$

$$
\begin{aligned}
p_i^*(t) =& \frac{1}{2}u_{\min}t^2 + e_i t + f_i, \\
v_i^*(t) =& u_{\min}t + e_i, \qquad\qquad \forall\ t \in [\tau_2^+, T_i^{m'}],
\end{aligned} \tag{2.114}
$$

where b_i, c_i, d_i, e_i and f_i are constants of integration, and time τ_1 and τ_2 are times that we move from one arc to another arc, which are found by using initial and final conditions in zone m and continuity of states at τ_1 and τ_2.

Case 3: CAV $i \in \mathcal{N}(t)$ enters the constrained arc $u_i(t) = u_{\min}$ at T_i^m. Then, it moves to the constrained arc $u_i(t) = u_{\max}$ at τ_1 and stays on it until T_i^{m+1}.

Theorem 2.1.24. *Let T_i^m and T_i^{m+1} be the schedules of CAV $i \in \mathcal{N}(t)$ for zones $m, m+1 \in \mathcal{I}_i$ respectively, where zone $m+1$ follows zone m. In zone m, the CAV i first travels in the constrained arc $u_i(t) = u_{\min}$ and then at the constrained arc $u_i(t) = u_{\max}$, if the speed constraint does not become active in zone m and*

$$T_i^{m+1} - T_i^m = D_i^m. \tag{2.115}$$

Proof. Let CAV $i \in \mathcal{N}(t)$ enter and and exit the zone $m \in \mathcal{I}_i$ at T_i^m and $T_i^{m'}$ respectively. substituting (2.10) into $T_i^{m+1} - T_i^m = D_i^m$, we have $T_i^{m'} - T_i^m = D_i^m$. Thus, CAV i is traveling at the latest feasible time in zone m. From Proposition (2.1.16), CAV i is decelerating with $u_{\min}$ and accelerating with $u_{\max}$ in zone m. □

In the latter case, the optimal control input is

$$u_i^*(t) = \begin{cases} u_{\min} & \text{, if} \quad T_i^m \le t < \tau_1 \\ u_{\max} & \text{, if} \quad \tau_1 \le t \le T_i^{m'} \end{cases}. \tag{2.116}$$

Substituting (2.116) in (2.2), we have

$$\begin{aligned} p_i^*(t) =& \frac{1}{2} u_{\min} t^2 + b_i t + c_i, \\ v_i^*(t) =& u_{\max} t + b_i, && \forall\ t \in [T_i^m, \tau_1^-], \end{aligned} \tag{2.117}$$

$$\begin{aligned} p_i^*(t) =& \frac{1}{2} u_{\max} t^2 + d_i t + e_i, \\ v_i^*(t) =& u_{\min} t + d_i, && \forall\ t \in [\tau_1^+, T_i^{m'}], \end{aligned} \tag{2.118}$$

where b_i, c_i, d_i and e_i are integration constants, which can be computed by using initial and final conditions of CAV in zone $m \in \mathcal{I}_i$ respectively. The switching point τ_1 can be found from (2.49).

Case 4: CAV i enters the constrained arc $u_i(t) = u_{\min}$ at T_i^m, then it moves to the constrained arc $v_i(t) = v_{\min}$ at $t = \tau_1$. It exits the constrained arc $v_i(t) = v_{\min}$ at $t = \tau_2$, and it enters the constrained arc $u_i(t) = u_{\max}$ and stays on it until T_i^{m+1}.

Corollary 2.1.25. *CAV $i \in \mathcal{N}(t)$ travels in zone $m \in \mathcal{I}_i$ as described at Case 4, if the speed constraint becomes active in zone m and (2.115) holds.*

Proof. As in Theorem (2.1.24), CAV i is traveling at the latest feasible time in zone m. From Proposition (2.1.21), the proof is complete. □

In the latter case, the optimal control input is

$$u_i^*(t) = \begin{cases} u_{\min} & \text{, if} \quad T_i^m \leq t < \tau_1 \\ 0 & \text{, if} \quad \tau_1 \leq t \leq \tau_2 \\ u_{\max} & \text{, if} \quad \tau_2 \leq t \leq T_i^{m'} \end{cases}. \tag{2.119}$$

Substituting (2.119) in (2.2), we have

$$\begin{aligned} p_i^*(t) =& \frac{1}{2}u_{\min}t^2 + b_i t + c_i, & & \\ v_i^*(t) =& u_{\min}t + b_i, & \forall\ t \in [T_i^m, \tau_1^-], & \quad (2.120) \\ p_i^*(t) =& v_{\min}t + d_i, & & \\ v_i^*(t) =& v_{\min}, & \forall\ t \in [\tau_1^+, \tau_2^-], & \quad (2.121) \\ p_i^*(t) =& \frac{1}{2}u_{\max}t^2 + e_i t + f_i, & & \\ v_i^*(t) =& u_{\max}t + e_i, & \forall\ t \in [\tau_2^+, T_i^{m'}]. & \quad (2.122) \end{aligned}$$

2.1.9.3 CAV travels on the combination of constrained and unconstrained arc

Using (2.103), we first start with the unconstrained solution of Problem 2.1.12. If the solution violates any of the speed (2.4) or control (2.3) constraints, then the unconstrained arc is pieced together with the arc corresponding to the violated constraint at unknown time τ_1, and we re-solve the problem with the two arcs pieced together.

The two arcs yield a set of algebraic equations, which are solved simultaneously using the boundary conditions and interior conditions at τ_1. If the resulting solution violates another constraint, then the last two arcs are pieced together with the arc corresponding to the new violated constraint, and we re-solve the problem with the three arcs pieced together at unknown times τ_1 and τ_2. The three arcs will yield a new set of algebraic equations that need to be solved simultaneously using the boundary conditions and interior conditions at τ_1 and τ_2. The process is repeated until the solution does not violate any other constraints; see [24].

2.1.9.4 CAV enters the safety constrained arc

Let CAV i enter and exit zone $m \in \mathcal{I}_i$ at T_i^m and $T_i^{m'}$ respectively. CAV k is immediately positioned in front of CAV i in zone m, and CAV i activates the rear-end safety constraint (2.6) at time $\tau_1 \in [T_i^m, T_i^{m'}]$. We have two cases to consider: Case 1: CAV i remains in the constrained arc until $T_i^{m'}$ or Case 2: CAV i exits the constrained arc at $\tau_2 \in [\tau_1, T_i^{m'}]$.

Lemma 2.1.26. *Let CAV i and $k \in \mathcal{N}(t)$ enter the zone m at time T_i^m and T_k^m respectively, and CAV k is immediately ahead of CAV i. CAV i does not activate the rear-end safety constraint at the entry of zone m, if minimum time gap, h, in the upper-level control belongs to the following set*

$$\Gamma = \{t \mid \frac{1}{2}u_{\min}t^2 + v_k(T_k^m)t - \varphi v_i(T_i^m) - \gamma_i > 0, \ \forall\ t \in \mathbb{R}^+\}. \tag{2.123}$$

Proof. Let CAV $i \in \mathcal{N}(t)$ and $k \in \mathcal{N}(t)$ enter the zone m at T_i^m and T_k^m respectively, and CAV k is located in front of CAV i. Since CAV i and k are in the same lane and CAV k is in front, (2.11) simplifies to $T_i^m \geq T_k^m + h$. For CAV k we have

$$p_k(t) < p_k(t'), \quad \forall\ t < t' \in \mathbb{R}^+, \tag{2.124}$$

$$\inf(p_k(T_i^m)) = p_k(T_k^m + h), \quad T_i^m \geq T_k^m + h. \tag{2.125}$$

Evaluating the (2.6) at time T_i^m yields

$$(p_k(T_i^m) - d_k^{m,s}) - (p_i(T_i^m) - d_i^{m,s}) \geq \gamma_i + \varphi v_i(T_i^m). \tag{2.126}$$

Substituting $p_i(T_i^m) = d_i^{m,s}$ and $p_k(T_k^m) = d_k^{m,s}$ into (2.126) we have

$$(p_k(T_i^m) - p_k(T_k^m)) \geq \gamma_i + \varphi v_i(T_i^m), \tag{2.127}$$

$$(p_k(T_i^m) - p_k(T_k^m)) \geq \inf((p_k(T_i^m) - p_k(T_k^m))), \tag{2.128}$$

where

$$\inf((p_k(T_i^m) - p_k(T_k^m))) = p_k(T_k^m + h) - p_k(T_k^m). \tag{2.129}$$

If

$$p_k(T_k^m + h) - p_k(T_k^m) > \gamma_i + \varphi v_i(T_i^m) \tag{2.130}$$

holds, then (2.127) also holds, and the rear-end safety constraint never becomes active at $t = T_i^m$.

The LHS of (2.130) corresponds to the distance that CAV k travelled after h seconds from its entry in the zone m, denoted by $\Delta_k^m(h, u_i(t))$. Thus,

$$\underset{u_i(t)}{\operatorname{argmin}} \Delta_k^m(h, u_i(t)) = u_{\min}. \tag{2.131}$$

Substituting (2.131) and $t = h$ into (2.2), we have

$$\Delta_k^m = \frac{1}{2} u_{\min} h^2 + v_i(T_k^m) h \tag{2.132}$$

If (2.132) is greater than $\gamma_i + \varphi v_i(T_i^m)$, it yields (2.130), and the proof is complete. □

Lemma 2.1.27. *If the rear-end safety constraint becomes active for CAV $i \in \mathcal{N}(t)$ at $\tau_1 \in (T_i^m, T_i^{m'})$, then it must exit the rear-end safety constrained arc at $\tau_2 \in [\tau_1, T_i^{m'})$.*

Proof. From Lemma 2.1.26, it follows that CAV i with a schedule $T_i^m \in \mathcal{T}_i$ does not activate the rear-end safety constraint at the entry of zone m for all $m \in \mathcal{I}_i$. Since the exit time of zone m is $T_i^{m'} = T_i^{m+1}$, it does not activate the rear-end safety constraint at the exit of zone m. Thus, if CAV i activates the rear-end safety constraint at τ_1, it must exit the constrained arc before it exits zone m. □

2.1.9.4.1 Hamiltonian analysis when only rear-end safety is active

The Hamiltonian (2.102) when CAV $i \in \mathcal{N}(t)$ enters the rear-end safety constrained arc simplifies to the following.

$$\begin{aligned} H_i(t, p_i(t), v_i(t), u_i(t)) &= \frac{1}{2}u_i(t)^2 + \lambda_i^p v_i(t) + \lambda_i^v u_i(t) \\ &+\mu_i^s(t)(S^{(1)}(x_i(t), u_i(t))), \end{aligned} \tag{2.133}$$

where

$$S^{(1)}(x_i(t), u_i(t)) = v_i(t) - v_k(t) + \varphi u_i(t). \tag{2.134}$$

From the Euler-Lagrange equations we have

$$\dot{\lambda_i^p} = -\frac{\partial H_i}{\partial p_i} = 0, \tag{2.135}$$

$$\dot{\lambda_i^v} = -\frac{\partial H_i}{\partial v_i} = -\lambda_i^p - \mu_i^s, \tag{2.136}$$

$$\frac{\partial H_i}{\partial u_i} = 0 \text{ or } u_i = -\lambda_i^v - \mu_i^s \varphi. \tag{2.137}$$

Since the rear-end safety constraint is active, taking the time derivative of (2.134) we have

$$\dot{u_i}(t) + \frac{1}{\varphi}u_i(t) - \frac{1}{\varphi}u_k(t) = 0. \tag{2.138}$$

Considering $u_k(t) = a_k t + b_k$ and solving (2.138) for $u_i(t)$ yields

$$u_i(t) = a_k t + b_k - a_k \varphi + C_1 \exp\left(-\frac{t}{\varphi}\right). \tag{2.139}$$

Using (2.139) and solving (2.135)-(2.137), we have the following results for λ_i^v, λ_i^p and μ_i^s

$$\lambda_i^p(t) = C_2, \tag{2.140}$$

$$\mu_i^s(t) = a_k - C_2 - \frac{C_1}{2\varphi}\exp\left(-\frac{t}{\varphi}\right) + C_3 \exp\left(\frac{t}{\varphi}\right), \tag{2.141}$$

$$\lambda_i^v(t) = C_4 - a_k t - \frac{C_1}{2}\exp\left(-\frac{t}{\varphi}\right) - C_3\varphi\exp\left(\frac{t}{\varphi}\right). \tag{2.142}$$

Substituting (2.139) into (2.2) we have

$$v_i(t) = \frac{1}{2}a_k t^2 + b_k t - a_k\varphi t - C_1\varphi\exp\left(-\frac{t}{\varphi}\right) + e_i, \tag{2.143}$$

$$p_i(t) = \frac{1}{6}a_k t^3 + \frac{1}{2}b_k t^2 - \frac{1}{2}a_k\varphi t^2 + C_1\varphi^2\exp\left(-\frac{t}{\varphi}\right) + e_i t + f_i, \tag{2.144}$$

where e_i, f_i, C_1, C_2, C_3 and C_4 are constants of integration.

2.1.10 Simulation results

To evaluate the effectiveness of the proposed framework, we investigate the coordination of 16 vehicles. We consider two symmetrical intersections, where the length of each road connecting to the intersections is 300 m, and the length of the merging zones is 30 m. The minimum time headway is 1 s. The maximum acceleration limit is set to 1 m/s^2 and the minimum deceleration limit is -1 m/s^2. The CAVs enter the control zones from four different paths (Fig. 2.2) at random time with uniform distribution between 0 and 20 s. The desired speed at the boundary is set to 20 m/s. Standstill distance and reaction time are set to 5 m and 0.2 s. Upon arriving in the control zone, each CAV solves the upper-level scheduling problem the solution of which designates the optimal time of entry to each zone minimizing the CAV's total travel time.

We present the resulting schedule tuple of each CAV in Table 2.1. It can be seen from Table 2.1 that the framework does not limit only one CAV in the merging zones. For example, CAV 2 enters zone 4 at 14.06 s and exit the merging zone at 14.8 s. CAV 3 enters the merging zone at 14.3 s, while CAV 2 is already in the merging zone. Furthermore, CAV 3 enters the zone 4 at 15.06 s and activates the safety constraint (2.11) at the entry of zone 4 with CAV 2. Moreover, the relative position of CAV 2 and CAV 3 is shown in Fig. 2.3 for zones which rear-end collision may occur.

Table 2.1: Computed Schedules for sixteen CAVs

Path 1

Index	$t_i^0 = T_i^{22}$	T_i^5	T_i^7	T_i^{17}	t_i^f
1	0	12.01	12.75	13.49	25.50
5	5.75	18.80	19.54	20.28	32.29
9	11.33	23.34	24.08	24.82	36.83
13	13.27	25.38	26.12	26.86	38.87

Path 2

Index	$t_i^0 = T_i^{12}$	T_i^4	T_i^{13}	T_i^7	T_i^8	T_i^{19}	t_i^f
2	2.05	14.06	14.80	27.72	28.46	29.20	41.21
6	7.40	19.41	20.15	33.07	33.81	34.55	46.56
10	11.36	23.37	24.11	37.03	37.77	38.51	50.52
14	13.89	25.90	26.64	39.56	40.30	41.04	53.05

Path 3

Index	$t_i^0 = T_i^{10}$	T_i^3	T_i^4	T_i^{13}	T_i^7	T_i^8	T_i^{19}	t_i^f
3	2.16	14.30	15.06	15.80	28.72	29.46	30.20	42.21
7	9.32	21.33	22.07	22.81	35.73	36.47	37.21	49.22
11	12.12	24.13	24.87	25.61	38.53	39.27	40.01	52.02
15	13.98	26.14	26.90	27.64	40.56	41.30	42.04	54.05

Path 4

Index	$t_i^0 = T_i^{18}$	T_i^8	T_i^6	T_i^5	T_i^{14}	T_i^2	T_i^1	T_i^3	T_i^{11}	t_i^f
4	4.31	16.32	17.06	17.80	18.54	31.46	32.20	32.94	33.68	45.69
8	10.89	22.90	23.64	24.38	25.12	38.04	38.78	39.52	40.26	52.27
12	13.01	25.02	25.76	26.50	27.24	40.16	40.90	41.64	42.38	54.39
16	16.97	30.46	31.20	31.94	32.68	45.60	46.34	47.08	47.82	59.83

The upper-level control provides (2.11). For instance, CAV 13 and 2 enter the control zone at 13.27 s and 2.05 s respectively. However, CAV 13 enters the zone 7 earlier than CAV 2, CAV 2 should enter the zone 7 earlier than CAV 13, since it arrives earlier to the control zone.

The control input of CAV 15 for its first two zones is shown in Fig. 2.4. According to Theorem 2.1.24, CAV 15 follows $u_{\min}$ and then $u_{\max}$ trajectory in zone 3. It is shown that the unconstrained trajectory for the zone 10, (shown in black) violates

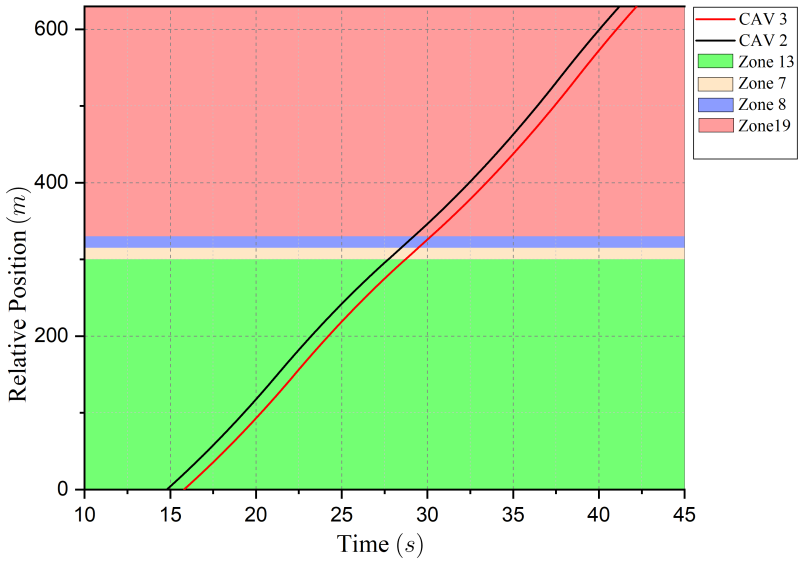

Figure 2.3: Relative Position of CAV 2 and CAV 3 in zones which rear-end collision may occur.

the $u_{\min}$ in $t \in [T_{15}^{10}, T_{15}^{3}]$, thus we pieced unconstrained and corresponding constrained arcs for zone 10, and the resulting trajectory is shown in Fig. 2.4 (in red).

The control input of CAV 13 for its first zone is shown in Fig. 2.5. CAV 13 violates the $u_{\min}$ in $t \in [T_{13}^{22}, T_{13}^{5}]$ (shown in black). We piece unconstrained arc and corresponding constrained arc for zone 22, and the resulting trajectory is shown in Fig. 2.5 (in red). As it can be seen, the resulting trajectory violates the $u_{\max}$ at the beginning. Thus, we piece constrained arc, $u_{\max}$, the unconstrained arc, and the constrained arc, $u_{\min}$, together. The final trajectory is shown in Fig. 2.5 (in blue), which does not violate any of the constraints.

The speed for the CAV $13 - 16$ is shown in Fig. 2.6. The relative positions for the CAVs travelling in zone 13 is shown in Fig. 2.7.

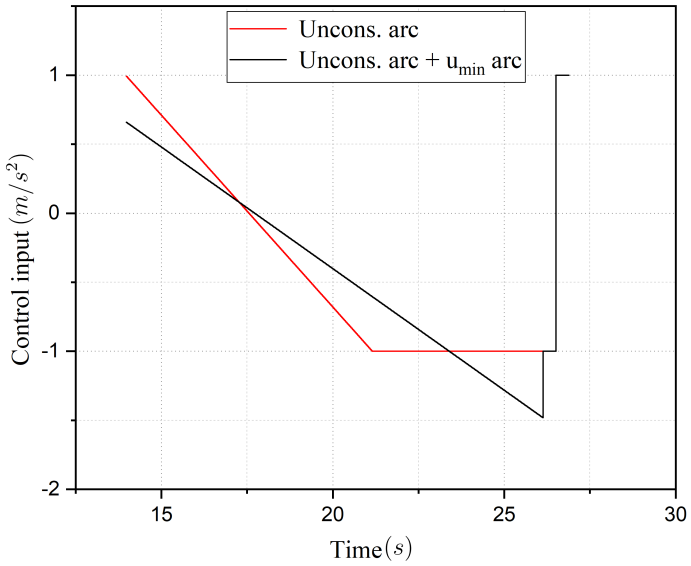

Figure 2.4: Control input profile of CAV 15 for zones 10 and 3.

2.2 Experimental Validation of a Real-Time Optimal Controller for Coordination of CAVs in a Multi-Lane Roundabout

In this section, we validate an optimal control algorithm developed earlier in a multi-lane roundabout scenario using University of Delaware's scaled smart city (UDSSC). We first provide conditions where the solution is optimal. Then, we demonstrate the feasibility of the solution using experiments at UDSSC, and show that the optimal solution completely eliminates stop-and-go driving while preserving safety.

2.2.1 Problem Formulation

In this section, we consider a multi-lane roundabout with three CAV inflows and three areas where lateral collisions between CAVs may occur; this is visualized in Fig. 2.8. To navigate the roundabout, we define a *control zone*, which starts upstream from the roundabout and ends at each roundabout exit. The control zone has an associated

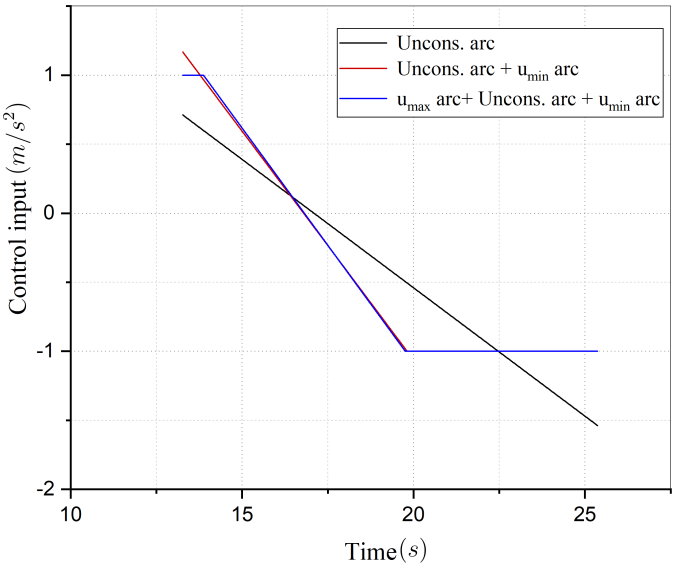

Figure 2.5: Control input profile of CAV 13 for zones 22 and 5.

coordinator, which stores information about the geometry of the roundabout and the trajectory information of each CAV in the control zone. The coordinator does not make any decisions and only acts as a database.

Let $\mathcal{N}(t) \subset \mathbb{N}$ be the set of CAVs at time $t \in \mathbb{R}^+$ which are inside the control zone. Upon entering the control zone at time $t_i^0 \in \mathbb{R}^+$, CAV $i \in \mathcal{N}(t)$ retrieves the trajectory information of every other CAV $j \in \mathcal{N}(t) \setminus \{i\}$ and generates an energy-optimal safe trajectory through the control zone. Then, CAV i broadcasts its trajectory to the coordinator. Finally, when CAV i exits the control zone at time t_i^f, it is removed from the set $\mathcal{N}(t)$. A detailed discussion of this coordinator framework is presented in [22].

Definition 2.2.1. *We define each lateral node with a unique index, $n \in \{1, 2, 3\}$, at each area inside the roundabout where there is potential for a lateral collision (Fig. 2.8).*

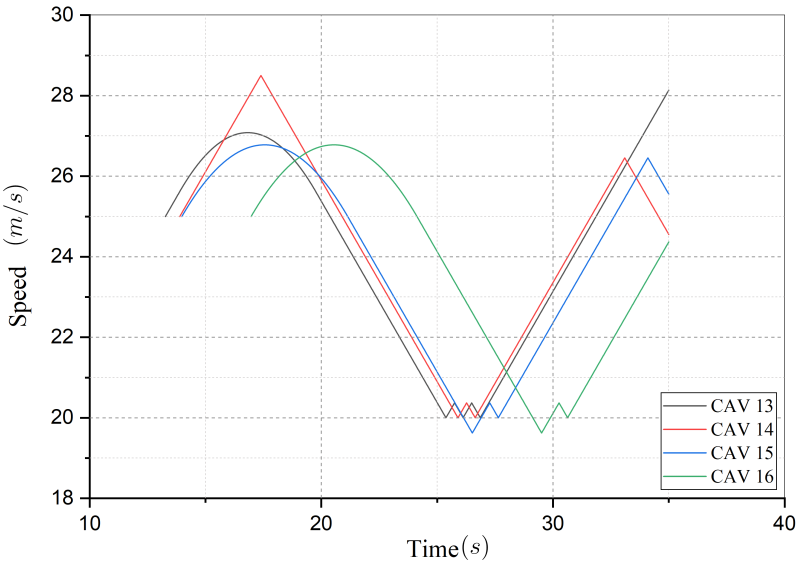

Figure 2.6: Speed profile of CAV $13 - 16$

Definition 2.2.2. *For each CAV $i \in \mathcal{N}(t)$, we define $\mathcal{C}_i$ as the set of all lateral nodes on the path of CAV i.*

For instance, if CAV i is traveling along path 1 (Fig. 2.8), the set of collision nodes is $\mathcal{C}_i = \{2, 3\}$

Definition 2.2.3. *For each CAV $i \in \mathcal{N}(t)$, upon entering the control zone at time t_i^0, we define the set of lateral nodes shared with each CAV $j \in \mathcal{N}(t_i^0) \setminus \{i\}$ as,*

$$\mathcal{C}_{i,j} = \{n \mid n \in \mathcal{C}_i \cap \mathcal{C}_j, \}. \tag{2.145}$$

2.2.2 CAV Model and Constraints

We represent the dynamics of each CAV $i \in \mathcal{N}(t)$, with the state equation and initial condition

$$\dot{\mathbf{x}}_i(t) = f(t, \mathbf{x}_i(t), u_i(t)), \qquad \mathbf{x}_i(t_i^0) = \mathbf{x}_i^0, \tag{2.146}$$

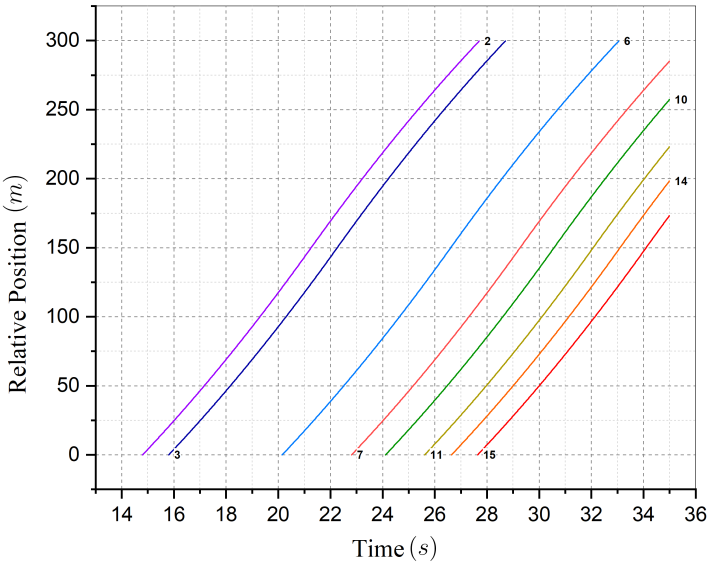

Figure 2.7: Relative Position of CAVs travelling in zone 13.

where $t \in \mathbb{R}^+$, and $\mathbf{x}_i(t) = [p_i(t), v_i(t)]^T$, $u_i(t)$ are the state and control input of i at time t. Let t_i^0 be the time that i enters the control zone, and $\mathbf{x}_i^0 = [p_i^0, v_i^0]^T$ be the state at this time. We model each CAV i as a double integrator

$$\begin{aligned} \dot{p}_i &= v_i(t), \\ \dot{v}_i &= u_i(t), \end{aligned} \tag{2.147}$$

where $p_i(t) \in \mathcal{P}_i$, $v_i(t) \in \mathcal{V}_i$, and $u_i(t) \in \mathcal{U}_i$ denote the position, speed and acceleration/deceleration (control input) of each CAV i inside the control zone. The sets $\mathcal{P}_i$, $\mathcal{V}_i$, and $\mathcal{U}_i$ are complete and totally bounded subsets of $\mathbb{R}$.

For each CAV $i \in \mathcal{N}(t)$ the control input and speed at time $t \in [t_i^0, t_i^f]$ are bounded by

$$\begin{aligned} u_{i,min} \leq u_i(t) \leq u_{i,max}, \\ 0 < v_{\min} \leq v_i(t) \leq v_{\max}, \end{aligned} \tag{2.148}$$

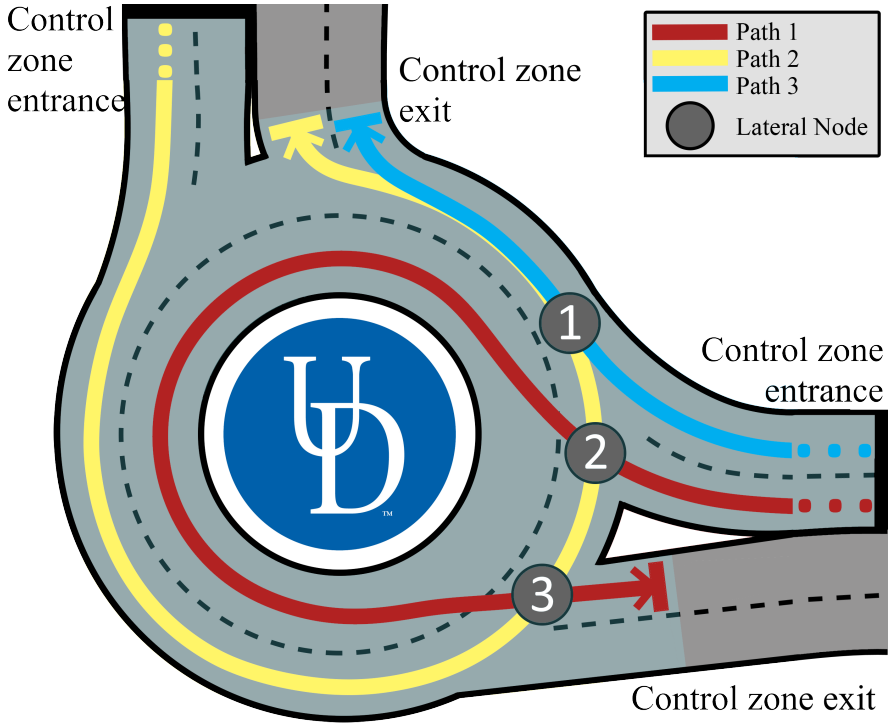

Figure 2.8: A schematic of the roundabout scenario. The highlighted control zone continues upstream from the roundabout. There are three conflict points which may result in lateral collisions.

where $u_{i,min}$, $u_{i,max}$ are the minimum deceleration and maximum acceleration for each i inside the control zone, and $v_{\min}$, $v_{\max}$ are the minimum and maximum speed limits respectively. For simplicity, we do not consider CAV diversity. Thus, in the rest of the paper, we set $u_{i,min} = u_{\min}$ and $u_{i,max} = u_{\max}$.

Definition 2.2.4. *For any CAV $i \in \mathcal{N}(t)$, if there exists a CAV $k \in \mathcal{N}(t)$ which leads CAV i, we define $d_i(t)$ as the bumper-to-bumper distance from CAV k to CAV i. If no such CAV k leads CAV i, then we let $d_i(t) \to \infty$.*

To guarantee no rear-end collision occurs between CAV $i \in \mathcal{N}(t)$ and the preceding CAV $k \in \mathcal{N}(t)$, we impose the following rear-end safety constraint,

$$d_i(t) \geq \delta_i(t), \tag{2.149}$$

where $\delta_i(t)$ is a predefined safe distance. The minimum safe distance $\delta_i(t)$ is a function of speed,

$$\delta_i(t) = \gamma + \varphi\, v_i(t), \tag{2.150}$$

where $\gamma, \varphi \in \mathbb{R}$ are the standstill distance and reaction time, respectively.

Lemma 2.2.5. *For CAV $i \in \mathcal{N}(t)$ the inverse function of position, $p_i^{-1}(\cdot)$ exists for all $t \in [t_i^0, t_i^f]$.*

Proof. From (2.148), we have $v_i(t) > 0$ for $t \in [t_i^0, t_i^f]$, which implies that $p_i(t)$ is a strictly increasing function. Thus, $p_i(t)$ is an one-to-one function and its inverse exists. □

For each CAV $i \in \mathcal{N}(t)$ the distance to a node $n \in \mathcal{C}_i$ is denoted by the function $l_i : \mathcal{C}_i \to \mathcal{P}_i$. To guarantee lateral collision avoidance, we impose the following constraint for every CAV $i \in \mathcal{N}(t)$,

$$\begin{aligned} &\left|p_i^{-1}(l_i(n)) - p_j^{-1}(l_j(n))\right| > t_h, \\ &\forall\, n \in \mathcal{C}_{i,j}, \quad \forall\, j \in \mathcal{N}(t) \setminus \{i\}, \end{aligned} \tag{2.151}$$

where $t_h \in \mathbb{R}^+$ is a safe time headway.

Remark 2.2.6. *The lateral safety constraint, (2.151) relaxes the first-in-first-out policy between CAVs $i, j \in \mathcal{N}(t)$, which is common in the literature. We avoid this restriction by incorporating an absolute value into (2.151).*

Next, we formulate a decentralized optimal control problem for each CAV $i \in \mathcal{N}(t)$ in order to minimize their energy consumption over the interval $t \in [t_i^0, t_i^f]$.

Problem 2.2.7. *When a CAV $i \in \mathcal{N}(t)$ enters the control zone, it solves the following optimal control problem:*

$$\begin{aligned} \min_{u_i(t) \in \mathcal{U}_i} \quad & \tfrac{1}{2} \textstyle\int_{t_i^0}^{t_i^f} u_i^2(t)\ dt, \\ \text{subject to :} \quad & (2.147), (2.148), (2.149), (2.151), \\ \text{given} \quad & p_i(t_i^0), v_i(t_i^0),\ p_i(t_i^f). \end{aligned}$$

To derive the analytical solution of Problem 3.1.2, we follow the standard methodology used in optimal control problems with interior point state and control constraints [24, 81, 82]. First, we start with the unconstrained solution to Problem 3.1.2. If this solution violates any of the state or control constraints, then it is pieced together with the arc corresponding to the violated constraint. This yields a set of algebraic equations that are solved simultaneously using the boundary conditions of Problem 3.1.2 and interior conditions between the arcs. If the resulting solution, which incorporates the optimal switching time between arcs, violates another constraint, then the two arcs are pieced together with a third, which corresponds to the new constraint which has been violated. This yields a larger set of algebraic equations that must be solved simultaneously using the boundary conditions of Problem 3.1.2 and the interior point conditions between arcs, including the optimal time and state to switch between them. This process is repeated until a piecewise-continuous state trajectory is found, which is a feasible solution for Problem 3.1.2.

In general, there is no analytical expression for the solution of Problem 3.1.2 when a safety constrained arc becomes active. Additionally, finding a piecewise-continuous state trajectory that optimally pieces the different arcs together is very computationally challenging, and it may become prohibitively difficult for a CAV to solve the optimal control problem onboard in real time [66].

In our approach, we consider the unconstrained solution to Problem 3.1.2, i.e., the solution when the state, control, and safety constraints, are neglected. The optimal unconstrained trajectory in this case is [24],

$$p_i(t) = a_i t^3 + b_i t^2 + c_i t + d_i, \tag{2.152}$$

$$v_i(t) = 3a_i t^2 + 2b_i t + c_i, \tag{2.153}$$

$$u_i(t) = 6a_i t + 2b_i, \tag{2.154}$$

with the boundary conditions

$$p_i(t_i^0) = p_i^0, \quad v_i(t_i^0) = v_i^0, \tag{2.155}$$

$$p_i(t_i^f) = p_i^f, \quad u_i(t_i^0) = 0. \tag{2.156}$$

To derive an energy-optimal control input that can be computed in real time, we seek to minimize the exit time of CAV $i \in \mathcal{N}(t)$ from the control zone and impose (2.152) - (2.154) as an energy-optimal motion primitive. This results in a new energy-optimal scheduling problem [83].

Problem 2.2.8. *When a CAV $i \in \mathcal{N}(t)$ enters the control zone, it derives its minimum travel time such that the resulting trajectory is unconstrained and does not violate any state, control, or safety constraints.*

$$\begin{aligned} \min_{a_i, b_i, c_i, d_i} \quad & t_i^f, \\ \text{subject to:} \quad & (2.148), (2.149), (2.151), \\ & (2.152), (2.153), (2.154), (2.155), (2.156). \end{aligned}$$

Thus, each CAV $i \in \mathcal{N}(t)$ will follow the solution to Problem 2.2.8, which generates the minimum travel time and imposes the unconstrained energy-optimal trajectory. That is, the solution of Problem 2.2.8 yields the minimum t_i^f such that the generated trajectory is the unconstrained and optimal solution to Problem 3.1.2. Note that as (2.152) is a strictly-increasing cubic polynomial for all $t \in [t_i^0, t_i^f]$, the inverse position (2.151) has a closed-form representation [83]. Next, we provide the assumptions we imposed in our approach on each CAV $i \in \mathcal{N}(t)$.

Assumption 2.2.9. *There are no errors or delays in the vehicle-to-vehicle and vehicle-to-infrastructure communication.*

Assumption 2.2.10. *Vehicle-level control is handled by a low-level controller, which can perfectly track the trajectory generated by solving Problem 2.2.8.*

The first assumption ensures that we address the deterministic case. It is relatively straightforward to relax this assumption as long as the noise or delays are

bounded. The second assumption is to decouple the motion planning and vehicle control, which makes the problem tractable. By tuning the low-level controller, it can be ensured that the prescribed trajectory is followed.

2.2.3 Analytical solution

We seek to transform Problem 2.2.8 into an equivalent formulation which can be solved in real time. First, without loss of generality, we consider the domain of Problem 2.2.8 to be $t \in [0, t_i^f]$ and $p_i(t) \in [0, S_i]$, where S_i is the length of the control zone corresponding to CAV i's path. This results in a new set of boundary conditions,

$$p_i(t_i^0 = 0) = 0, \qquad v_i(t_i^0 = 0) = v_i^0, \tag{2.157}$$

$$p_i(t_i^f) = S_i, \qquad u_i(t_i^f) = 0. \tag{2.158}$$

Next, we substitute (2.157) into (2.152) and (2.153) yielding

$$p_i(t_i^0 = 0) = d_i = 0, \tag{2.159}$$

$$v_i(t_i^0 = 0) = c_i = v_i^0, \tag{2.160}$$

which must always hold for Problem 2.2.8. Next, we substitute (2.158) into (2.154), which yields,

$$u_i(t_i^f) = 6a_i t_i^f + 2b_i = 0. \tag{2.161}$$

This implies that

$$a_i = -\frac{b_i}{3t_i^f}. \tag{2.162}$$

Next, we substitute (2.158) and (2.162) into (2.152) yielding

$$p_i(t_i^f) = -\frac{b_i}{3t_i^f} {t_i^f}^3 + b_i {t_i^f}^2 + v_i^0 t_i^f = S_i. \tag{2.163}$$

Hence, equation (2.163) simplifies to

$$b_i = \frac{3(S_i - v_i^0 t_i^f)}{2{t_i^f}^2}. \tag{2.164}$$

We may further simplify Problem 2.2.8 by finding a compact domain of feasible t_i^f by explicitly applying the speed and control constraints. Let $t_{i,\min}^f$ and $t_{i,\max}^f$ denote the lower bound and upper bound on t_i^f respectively, which is imposed by the state and control constraints.

Proposition 2.2.11. *For each CAV $i \in \mathcal{N}(t)$, the lower bound on exit time of the control zone, $t_{i,\min}^f$, is computed as follows*

$$t_{i,\min}^f = \min\{t_{i,u_{\max}}^f, t_{i,v_{\max}}^f\}, \tag{2.165}$$

where

$$t_{i,u_{\max}}^f = \frac{\sqrt{9v_0^2 + 12S_i u_{\max}} - 3v_0}{2u_{\max}}, \tag{2.166}$$

$$t_{i,v_{\max}}^f = \frac{3S_i}{v_i^0 + 2v_{i,\max}}. \tag{2.167}$$

Proof. There are two cases to consider: **Case 1:** CAV i achieves its maximum control input at entry of the control zone, as $u_i(t_i^0) = u_{\max}$. **Case 2:** CAV i achieves its maximum speed at the end of control zone, as $v_i(t)$ is strictly increasing $v_i(t_i^f) = v_{\max}$.

In case 1, by (2.154), we have

$$u_i(t_i^0 = 0) = 2b_i = u_{\max}. \tag{2.168}$$

Substituting (2.164) into (2.168) and solving for t_i^f, yields the quadratic equation

$$u_{\max} {t_i^f}^2 + 3v_i^0 t_i^f - 3S_i = 0, \tag{2.169}$$

which has two real roots with opposite signs, as $t_{i,1}^f t_{i,2}^f = \frac{-3S_i}{u_{\max}} < 0$. Thus, $t_{i,u_{\max}}^f > 0$ is computed by

$$t_{i,u_{\max}}^f = \frac{\sqrt{9v_0^2 + 12S_i u_{\max}} - 3v_0}{2u_{\max}}. \tag{2.170}$$

For case 2, by (2.153), we have

$$v_i(t_i^f) = \frac{a_i}{3} {t_i^f}^2 + \frac{b_i}{2} t_i^f + v_i^0 = v_{\max}. \tag{2.171}$$

Substituting (2.162) and (2.164) into 2.171 yields

$$v_i(t_i^f) = 3\Big(\frac{-b_i}{3t_i^f}\Big){t_i^f}^2 + 2b_i t_i^f + v_0 \tag{2.172}$$
$$= b_i t_i^f + v_0 = \frac{3(S_i - v_i^0 t_i^f)}{2t_i^f} + v_0 = v_{\max},$$

which simplifies to

$$t_{i,v_{\max}}^f = \frac{3S_i}{v_i^0 + 2v_{\max}}. \tag{2.173}$$

Thus, our lower bound on t_i^f is given by

$$t_{i,\min}^f = \min\{t_{i,u_{\max}}^f, t_{i,v_{\max}}^f\}. \tag{2.174}$$

□

Proposition 2.2.12. *For each CAV $i \in \mathcal{N}(t)$, the upper bound on exit time of the control zone, $t_{i,\max}^f$, is computed as follows*

$$t_{i,\max}^f = \begin{cases} t_{i,v_{\min}} & , \text{ if } 9{v_i^0}^2 + 12S_i\ u_{\min} < 0, \\ \max\{t_{i,u_{\min}}^f, t_{i,v_{\min}}^f\} & , \text{otherwise.} \end{cases} \tag{2.175}$$

where

$$t_{i,v_{\min}} = \frac{3S_i}{v_i^0 + 2v_{\min}}, t_{i,u_{\min}} = \frac{\sqrt{9v_0^2 + 12S_i u_{\min}} - 3v_0}{2u_{\min}}. \tag{2.176}$$

Proof. Similar steps can followed to find the upper bound for t_i^f, $t_{i,\max}^f$.

First, to find $t_{i,u_{\min}}^f$, we have

$$u_{\min}{t_i^f}^2 + 3v_i^0 t_i^f - 3S_i = 0, \tag{2.177}$$

which has two positive roots if the discriminant is non-negative, as $t_{i,1}^f t_{i,2}^f = \frac{-3S_i}{u_{\min}} > 0$. Of these we will select the smaller one,

$$t_{i,u_{\min}}^f = \frac{\sqrt{9v_0^2 + 12S_i u_{\min}} - 3v_0}{2u_{\min}}. \tag{2.178}$$

Note that when $9v_0^2 + 12S_i u_{\min} < 0$ there is no real root of t_i^f which satisfies all of the boundary conditions simultaneously. Thus, the constraint $u(t_i^0) = u_{\min}$ can never become active if (2.178) is complex, and the lower bound is given by the $v_{\min}$ case. The proof for the $v_{\min}$ case is identical to Proposition 2.2.12 and is omitted. □

Finally, we may write an equivalent formulation of Problem 2.2.8, which optimizes a single variable, t_i^f over a compact set $[t_{i,\min}^f, t_{i,\max}^f]$.

Problem 2.2.13. *When CAV $i \in \mathcal{N}(t)$ enters the control zone it derives the minimum exit time such that the resulting unconstrained trajectory does not violate any safety constraints.*

$$\begin{aligned} & \min_{t_i^f} t_i^f, \\ \text{subject to:} \quad & (2.149), (2.151), \\ & (2.159), (2.160), (2.162), (2.164), \\ & t_i^f \in [t_{i,\min}^f, t_{i,\max}^f]. \end{aligned}$$

Problem 2.2.13 can be numerically solved in real time by each CAV $i \in \mathcal{N}(t)$ upon entering the control zone. In the next section, we describe our experimental testbed and the implementation of the proposed approach.

2.2.4 Experimental Setup

To experimentally validate our method, experiments were carried out in UDSSC, (Fig. 2.9) using nine scaled CAVs traveling along three different conflicting paths (Fig. 2.8). UDSSC is a 1:25 scale testbed designed to replicate real-world traffic scenarios and test cutting-edge control technologies in a safe and scaled environment. UDSSC is a fully integrated smart city, which can be used to validate the efficiency of control and learning algorithms and their applicability in hardware. It utilizes high-end computers, a VICON motion capture system, and a fleet of scaled CAVs (Fig. 2.10) to simulate a variety of centralized and decentralized control strategies. Each CAV has a Raspberry Pi 3B with a 1.2 GHz quad-core ARM processor and communicates with the *mainframe*

computer (Processor: Intel Core $i7-6950X$ CPU @ 3.00 GHz x 20, Memory: 125.8 Gb). UDSSC has been used successfully for coordination of CAVs [21,22] and implementation of reinforcement learning policies [84, 85].

Figure 2.9: The University of Delaware's scaled smart city. The roundabout used in this experiment is in the upper-left side of the image.

High-level routing is achieved by a multithreaded C++ application, which runs on the mainframe computer. The CAV receives its position, speed profile, and the path information from the mainframe and uses a modified Stanley [86] controller to handle lane tracking. Meanwhile, a feed-forward-feedback PID controller [87] tracks the desired speed profile. Medium and low-level control is accomplished on-board each CAV in a purely distributed manner. For further details about UDSSC's hardware, see [22].

Each CAV starts their path outside the control zone and applies the Intelligent Driver Model (IDM) [88]. The acceleration command given to a CAV $i \in \mathcal{N}(t)$ following

Figure 2.10: A picture of the connected and automated vehicles in University of Delaware's scaled smart city.

CAV $k \in \mathcal{N}(t)$ is

$$u_i = a_{\max}\left(1 - \left(\frac{v_i}{v_{\max}}\right)^{\delta} - \frac{s_0 + v_i t_h + \big(v_i(v_i - v_k)\big)^2}{2\sqrt{a_{\max} v_{\max}}\, d_i}\right)$$

where δ is the acceleration exponent, t_h is the desired time headway, and s_0 is the desired standstill distance.

Upon entering the control zone, CAV $i \in \mathcal{N}(t)$ determines its trajectory by solving Problem 2.2.13 numerically. CAV i, then, follows this fixed trajectory and returns to the IDM controller after exiting the control zone.

Table 2.2 gives the parameters used in the experiment such as control zone length, state and control constraints, (2.148), and safety constraints, (2.149), (2.151). The experiments in UDSSC used nine CAVs with three CAV per path (Fig. 2.8). The experiment was repeated five times to collect multiple data sets and give an estimate on the noise and disturbances present in the system. The CAV inflows were explicitly configured to lead to lateral collisions in the uncontrolled case. Next, we present and discuss the results of these experiments.

Table 2.2: Parameters used for the optimal controller in University of Delaware's scaled smart city; values are given in the 1:25 city scale.

Parameters	Values	Reference
S_1, S_2, S_3	5.36 m, 5.81 m, 3.78 m	Control zone lengths
$v_{\min}, v_{\max}$	0.15 m/s, 0.5 m/s	State constraints
$u_{\min}, u_{\max}$	-0.45 m/s^2, 0.45 m/s^2	Control constraints
γ, ϕ	1 m, 0.27 s	Rear-end safety (2.149)
t_h	1.0 s	Time headway (2.151)

2.2.5 Results and Discussion

To validate our proposed controller in UDSSC, several pieces of data were collected throughout the five experiments. First, the position, speed, location within the UDSSC, and a timestamp for each CAV was streamed back to the mainframe at a rate of 20 Hz. Furthermore, the state and time of each CAV entering the control zone were recorded, as well as the computed and achieved exit time. These results are summarized in Table 2.3. Note that the minimum speed of any CAVs across all five experiments is 0.12 m/s (7 mph at full scale), which demonstrates that stop and go driving has been completely eliminated. Additionally, the average CAV speed is 0.42 m/s (24 mph at full scale), which implies that most CAVs are traveling near $v_{\max}$ and must apply minimal control effort.

Table 2.3: Average velocity and travel time results for the 5 experiments. RMSE is normalized by travel time for each CAV.

Experiment	$v_{\min}$ [m/s]	v_{avg} [m/s]	Travel Time RMSE
1	0.16	0.41	2.71 %
2	0.27	0.45	1.54 %
3	0.18	0.41	4.03 %
4	0.12	0.43	1.92 %
5	0.21	0.42	1.38 %

The exit time data for each CAV is visualized in Fig. 2.11, where the grey bars represent the feasible space of t_i^f, the wide black bars correspond with the solution

of Problem 2.2.13, and the thin red bars show the achieved exit time for each CAV. From Table 2.3, the error between desired and actual exit time varies between 2-4%. This error comes from the CAV's ability to track the desired trajectory and shows that Assumption 2.2.10 is reasonable for well-tuned CAVs in UDSSC.

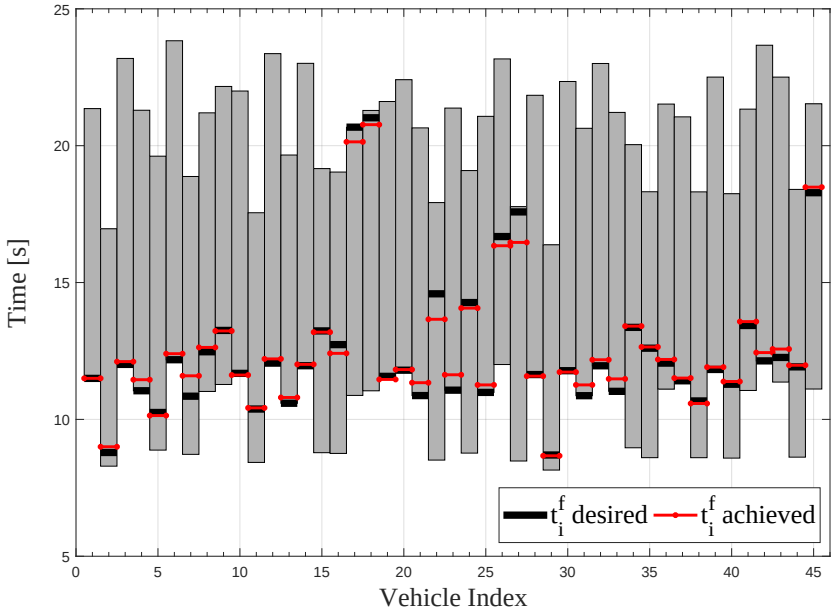

Figure 2.11: Estimated and actual arrival time for each CAV over all experiments. The grey bar shows the range of admissible t_i^f from the state and control constraints. Every 9 CAVs corresponds to a single experiment; they are sorted in ascending order by departure time from the control zone.

The position trajectory of an ego-CAV following path 2 is given in Fig. 2.12; the ego-CAV's position is denoted by the dashed red line, while the positions of two other CAVs are represented by dotted black lines. The lateral collision constraints are denoted by vertical black bars, and the rear-end safety constraint is the hashed region on the graph. There are two other CAVs shown; one is on Path 3 and merges in front of the ego-CAV at collision node 1 (Fig. 2.8) and the second CAV leads the ego-CAV on path 2.

Figure 2.12 demonstrates that for a real CAV Assumption 2.2.9 is too strong. The trajectory generated by the ego-vehicle may not violate any constraints, but the

actual trajectory violates the rear-end safety constraint by a car length (0.2 m). However, at this speed, the rear-end safety constraint requires a three-car length gap, so a robust control formulation of Problem 2.2.13 could likely guarantee collision avoidance. This can also be seen in the lateral collision avoidance constraint in Fig. 2.12, where a later CAV crosses node 3 in a way that violates the time headway constraint (again, without leading to an actual collision).

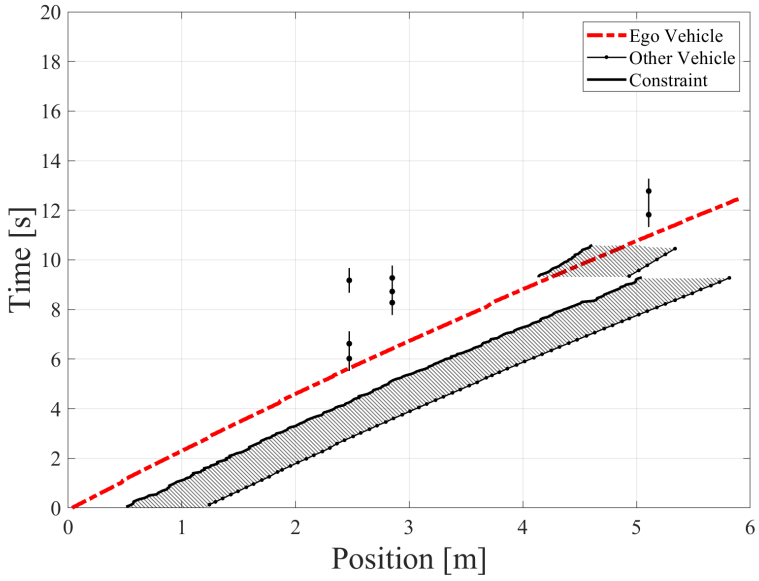

Figure 2.12: Position trajectory for the third CAV entering from path 2 in the 5th experiment. The lateral constraints are shown as vertical lines, and the rear-end safety constraint is the hashed region.

Finally, the average, maximum, and minimum speed for each CAV across all experiments are given in Figs. 2.13 - 2.15. Each figure corresponds to a single path (see Fig. 2.8) and is taken over 15 CAV (3 CAVs per path over five experiments). The CAVs' positions are taken directly from VICON and numerically derived using a first-order method.

From Figs. 2.13 - 2.15, the average speed for CAVs on each path is very close to constant. Path 1 shows the most variance, which is due to the distance between collision nodes 2 and 3 on path 1 (see Fig. 2.8). In order for a CAV $i \in \mathbb{Q}(t)$ which is

traveling along path 1 to reduce its arrival time at node 2, it must make a proportionally larger reduction in the value of t_i^f. This is a side effect of enforcing the unconstrained trajectory on each CAV over the entire control zone. Additionally, the entrance to the control zone along path 3 follows a sharp right turn. This results in a relatively lower average trajectories in Fig. 2.14, as the dynamics of the CAVs reduce their speed while rounding these turns, causing them to enter the control zone at a lower speed.

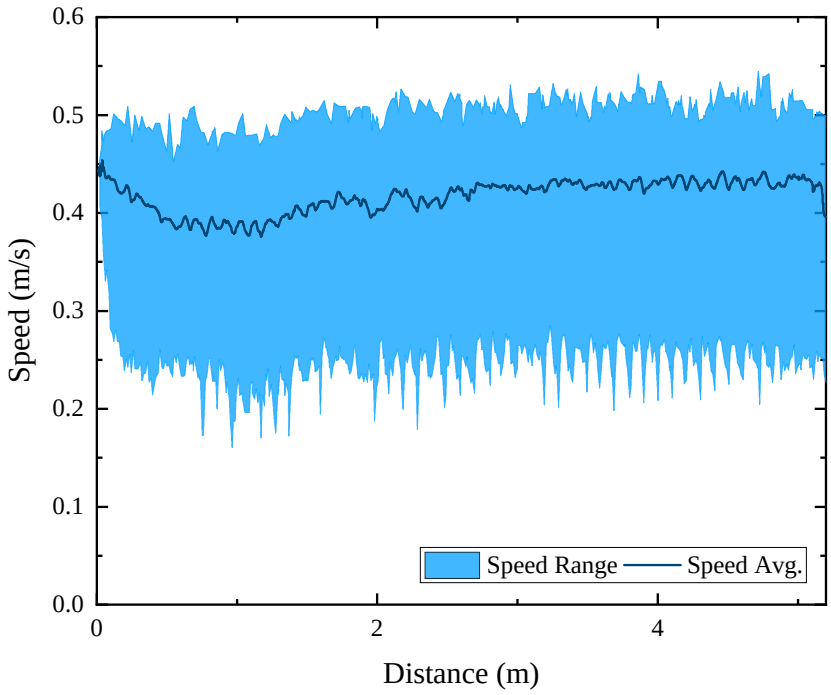

Figure 2.13: Maximum, minimum, and average speed of CAVs on the path 1 (Fig.2.8) over the control zone length for the five experiments.

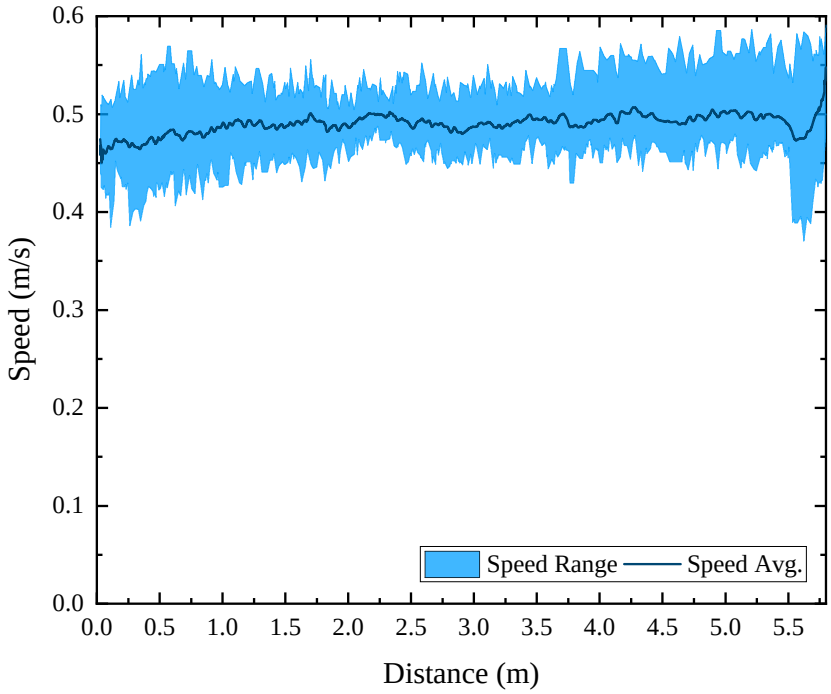

Figure 2.14: Maximum, minimum, and average speed of CAVs on the path 2 (Fig.2.8) over the control zone length for the five experiments.

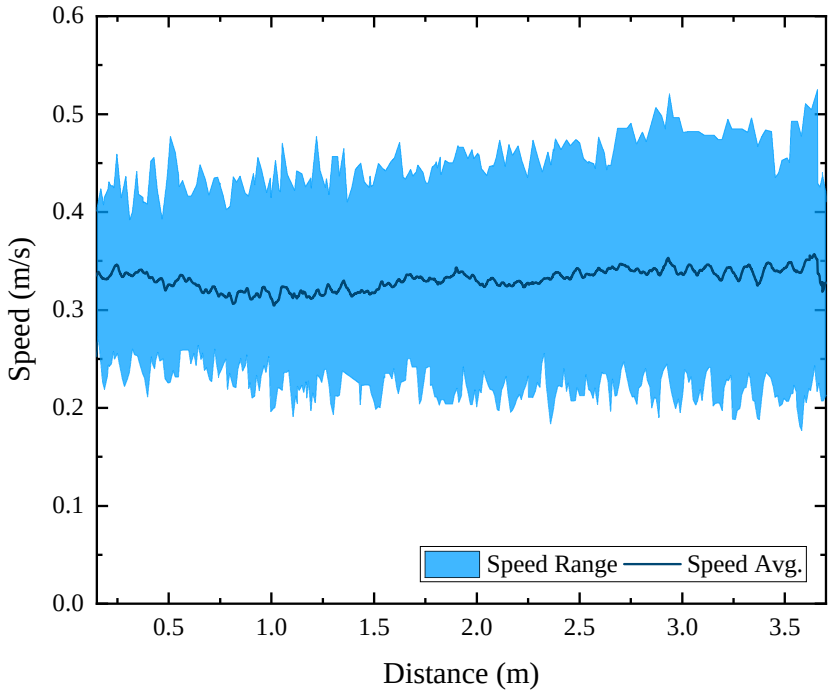

Figure 2.15: Maximum, minimum, and average speed of CAVs on the path 3 (Fig.2.8) over the control zone length for the five experiments.

Chapter 3

PROPOSED DISSERTATION RESEARCH

In the previous chapter, we presented some preliminary results that we developed for coordination of CAVs at multiple intersections and roundabouts, to smooth traffic flow and improve the fuel efficiency of each CAV while preserving safety. In our problem formulation, we imposed several assumptions. Namely, we assumed that there are no errors and/or delays in the vehicle-to-vehicle and vehicle-to-infrastructure communication. The latter enabled us to formulate the problem deterministically. We presented an optimal control framework for the deterministic constrained case, and we demonstrated the efficacy of the approach both through simulation and experiments in University of Delaware's scaled smart city testbed. However, during the experimental validations, we observed that neglecting uncertainty is a strong assumption. This is because the actual position trajectory of each CAV differs from the optimal planned trajectory due to the presence of uncertainties in the system. In addition, we noticed that the discrepancy between the experimental and optimal position trajectories led, in some instances, to the violation of the safety constraints for some CAVs. To avoid these situations in real-world scenarios, our optimization framework should guarantee either strict or high probability satisfaction of constraints in the system. Although using a feedback controller (or implementing the control algorithms for a receding horizon) may provide a certain level of robustness against noise and errors, the deterministic framework does not explicitly incorporate uncertainties in the model dynamics and observations. Therefore, uncertainties can affect the system evolution and might result in constraint violations or even sub-optimal performance [67, 89].

The overarching goal of this dissertation is to advance the state of the art in the area of coordination of CAVs and to establish an online stochastic optimal control framework for coordinating CAVs at traffic scenarios, e.g., merging at roadways, intersections, roundabouts, and speed reduction zones with imperfect state information and delayed communication while guaranteeing safety. We will accomplish this goal by addressing the following three specific aims: (1) develop a stochastic optimal control framework for coordinating CAVs that accounts for disturbances in the system, (2) enhance the framework to consider imperfect state information and noisy state observation, and (3) extend the outcome of aims 1 and 2 to include delays in the communication. Next, we discuss the research plan towards achieving these aims.

3.1 Research plan

Aim 1: To accomplish our first aim, we propose to model uncertainties as Brownian motion and integrate them into the CAV's dynamics model. There are numerous sources of uncertainties in the system, including model mismatch, disturbances from the environment, and tracking error in the vehicle control block. We will follow the hierarchical approach discussed in prior work [90] (Chapter 2). Namely, coordination of CAVs will be decomposed into two levels. In the upper-level, we will formulate a scheduling problem, the solution of which designates the optimal time for each CAV to exit the control zone while satisfying the lateral safety constraint. In the low-level, we will formulate an optimal control problem, the solution of which yields the optimal control input of each CAV to exit the control zone at the time specified by the upper-level scheduling problem. Although our proposed framework can be applied to any particular traffic scenario, e.g., merging roadways, roundabouts, intersections, and speed reduction zones, we refer to an intersection (Fig. 3.1), to provide the fundamental ideas of our proposed approach. We consider a single intersection shown in Fig. 3.1. A drone stores information about the geometric parameters of the roads, the paths of the CAVs, and schedules of CAVs. The intersection has a "control zone"

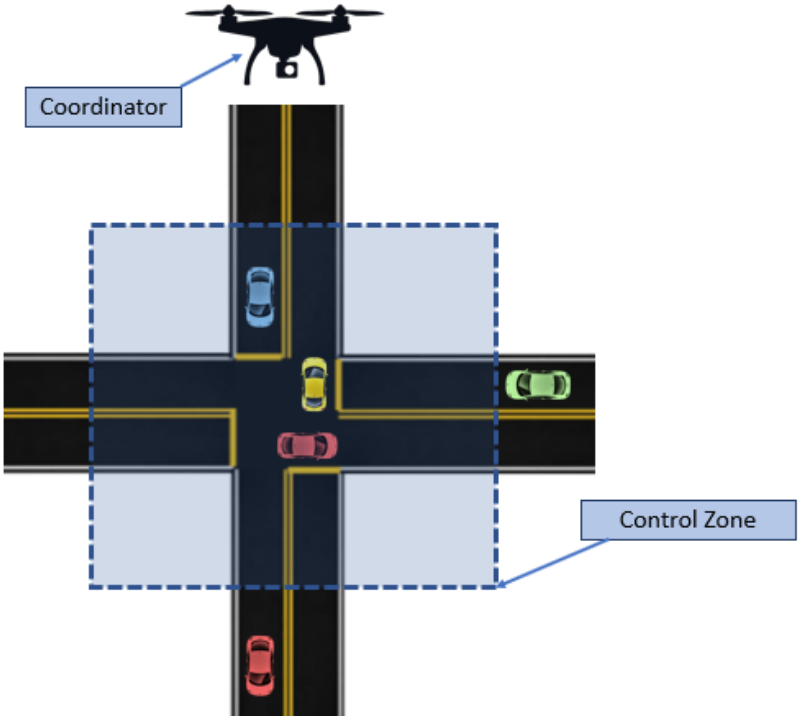

Figure 3.1: Single intersection with control zone and a drone acting as a coordinator

inside of which the drone can communicate with the CAVs. The drone does not make any decisions, and it only acts as a "database" for the CAVs. We define the area where lateral collisions may occur as a "merging zone." Let $N(t) \in \mathbb{N}$ be the number of CAVs inside the control zone at time $t \in \mathbb{R}^+$ and $\mathcal{N}(t) = \{1, \dots, N(t)\}$ be the queue that tracks the order that each CAV enters the control zone.

We will use the following stochastic equation to represent the dynamics of CAV $i \in \mathcal{N}(t)$ in a continuous space:

$$\begin{aligned} \mathrm{d}\mathbf{x}_i(t) &= \overbrace{f(t, \mathbf{x}_i(t), \mathbf{u}_i(t))\mathrm{d}t}^{\text{Drift}} + \overbrace{\sigma(t, \mathbf{x}_i(t), \mathbf{u}_i(t))\mathrm{d}W(t)}^{\text{Diffusion}}, \\ \mathbf{x}_i(t_i^0) &= \mathbf{x}_i^0, \end{aligned} \tag{3.1}$$

where $\mathbf{x}_i(t) = [p_i(t), v_i(t)]^{\mathrm{T}}$, $u_i(t)$ are the state and control input of CAV i at time t, where $p_i(t) \in \mathcal{P}_i$, $v_i(t) \in \mathcal{V}_i$, and $u_i(t) \in \mathcal{U}_i$ denote the position, speed and control input of each CAV i inside the control zone. The sets $\mathcal{P}_i$, $\mathcal{V}_i$, $\mathcal{U}_i$, and $i \in \mathcal{N}(t)$, are complete

and totally bounded subsets of $\mathbb{R}$. Let t_i^0 and t_i^f be the time that CAV $i \in \mathcal{N}(t)$ enters and exits the control zone. The first term in (3.1), $f(\cdot)$, is called a drift coefficient and represents the deterministic evolution of the system. The second term, $\sigma(\cdot)$, is called diffusion portion and models uncertainties and noise in the system with zero-mean m-dimensional Brownian motion $W(t)$. We will use linear models to describe both drift and diffusion process. As Bertnorp et al. [91] described, the control architecture of CAVs has at least two sub-components, which are motion planning and vehicle control. Motion planning, or a trajectory planner, determines a reference trajectory that a CAV should follow, and the vehicle control block that tracks the trajectories prescribed by the motion planner. Since our focus is on motion planning, choosing a linear model, such as a double integrator, will enable us to find a solution that can be implemented in real time. On the other hand, considering a more sophisticated model, which precisely captures the behavior of a CAV may be implausible due to computational burden and real-time implementation.

For each CAV $i \in \mathcal{N}(t)$ the control input and speed are bounded with the following constraints

$$u_{i,min} \leq u_i(t) \leq u_{i,max}, \tag{3.2}$$

$$0 < v_{\min} \leq v_i(t) \leq v_{\max}, \tag{3.3}$$

where $u_{i,min}, u_{i,max}$ are the minimum and maximum control inputs for each CAV $i \in \mathcal{N}(t)$ and $v_{\min}, v_{\max}$ are the minimum and maximum speed limit respectively. Additionally, for each CAV i, we also consider rear-end and lateral safety constraints.

Problem 3.1.1. *When a CAV $i \in \mathcal{N}(t)$ enters the control zone, it solves the following scheduling problem:*

$$\begin{aligned} &\min_{t_i^f \in \mathbb{R}^+} && t_i^f, \\ &\text{subject to :} && (3.1), (3.2), (3.3), \text{lateral safety} \\ &\text{given} && \mathbf{x}_i(t_i^0) = [p_i(t_i^0), v_i(t_i^0)]^{\mathrm{T}},\ p_i(t_i^f). \end{aligned}$$

Problem 3.1.2. *When a CAV $i \in \mathcal{N}(t)$ enters the control zone, it solves the following stochastic optimal control problem:*

$$\begin{aligned} \min_{u_i(t)\in\mathcal{U}_i} \quad & \tfrac{1}{2}\,\mathbb{E}[\int_{t_i^0}^{t_i^f} u_i^2(t)\ \mathrm{d}t], \\ \text{subject to}: \quad & (3.1), (3.2), (3.3), \text{rear-end safety} \\ \text{given} \quad & \mathbf{x}_i(t_i^0) = [p_i(t_i^0), v_i(t_i^0)]^{\mathrm{T}}\ ,\ p_i(t_i^f). \end{aligned}$$

Both the upper-level (Problem 3.1.1) and low-level problems (Problem 3.1.2) are constrained problems. We classify the constraints of the problems in two groups: (1) the hard constraints and (2) the soft constraints. Hard constraints, e.g., lateral safety, are the constraints that we want to strictly satisfy. In contrast, soft constraints, e.g., rear-end safety, state and control input constraints, are those that we can allow some violation within a predetermined threshold. To address hard constraints, we will use a robust control technique that utilizes the worst-case scenario. However, this yields a conservative solution, or it may have no feasible solution that strictly satisfies the constraint [69]. On the other hand, for the soft constraints, we can employ a chance-constrained approach which requires the violation of probability of all constraints to be bellow a designated threshold called a risk parameter [72]. Due to the probabilistic formulation of the chance-constrained problem, one possible approach is to tighten the constraint and translate it from a probabilistic constraint to an affine constraint [68,72].

To solve the stochastic optimal control problem, we will use Pontryagin's maximum principle and derive necessary and sufficient conditions for optimality [92–94]. An alternative approach that we plan to consider is formulating the Hamiltonian-Jacobi-Bellman equation and solving it using dynamic programming [67]. Although deriving a solution in real time with dynamic programming is not feasible, this solution will help us benchmark the optimal behavior and then use other methods, e.g., reinforcement learning, for real-time implementation.

Aim 2: In this aim, we seek to develop a decentralized control framework for

coordination of CAVs in different traffic scenarios, including merging roadways, roundabouts, intersections, and speed reduction zones, with imperfect state information and noisy observations. The first step in addressing Aim 2 is modeling noisy in the observations. We will model the observation of each CAV's state using the following linear equation

$$y_i(t) = Hx_i(t) + V(t), \tag{3.4}$$

where we assume that we fully observe the state of the system, $\mathbf{x}_i(t) = [p_i(t), v_i(t)]^{\mathrm{T}}$, and $H = \begin{bmatrix} 1 & 0 \\ 0 & 1 \end{bmatrix}$. Let $V(t) \in \mathbb{R}^2$ be the external observations disturbances.

A classic approach to address this aim is using a constrained linear quadratic Gaussian controller, due to the linearities in the model and constraints, and quadratic cost function. Lim et al. [95, 96] showed that in constrained linear quadratic problems with additive Gaussian noise, the separation principle holds. The latter can aim the optimal feedback control and the state estimation to be handled independently. To achieve this, we need to design an observer to estimate noisy states of the system at each time instant. To address the estimation problem, we will use a continuous version of the Kalman filter called Kalman-Bucy filter [89, 97]. Using the optimal feedback policy achieved from Aim 1, we will implement the policy using estimated states by a Kalman-Bucy filter. The limitations of the latter lie in the assumption of Gaussian noise and linear observation model. For a nonlinear observation model, we can use an extended Kalman filter [98], in which local linearization of the observation model will be performed. Relaxing the hypothesis of Gaussian noise can be conducted by using techniques such as particle filtering.

A second approach to Aim 2 is using data-driven methods, e.g., machine learning, to learn about the noise in the observations. Berkenkamp and Schoellig [99] used Gaussian process regression based on data gathered during the operation to update the initial model of their system. Embedding the data-based update in a robust control

framework, they guaranteed stability during the learning process. A similar idea can be employed to update the observation model as CAVs driving in the control zone.

Aim 3: In this aim, we seek to advance the state of the art in the field of decentralized coordination of CAVs at different traffic scenarios by considering delays in communication. Upon entering the control zone, CAVs communicate with other CAVs or infrastructure using vehicle-to-vehicle (V2V) and vehicle-to-infrastructure (V2I) communication. In our approach, to address delays in V2V or V2I communication, we will consider the problem as a retarded optimal control problem. Assuming that delays in the transportation network are constants, we will use Pontrayagyn's maximum principle to derive the optimal control policy of each CAV. This approach requires knowledge related to the constant or multiple delays over the state and control a priori [100–102]. To address this, we may need to include an online learning algorithm to learn the delays in the communication, and use that to derive necessary and sufficient conditions for the retarded optimal control problem.

An alternative approach to address Aim 3 is to assume unknown time delays. This entails modeling time delays as imaginary disturbances of the system. Addressing Aim 3 through this technique requires the completion of Aim 1. Zhang et al. [103] proposed designing a disturbance observer over the system with unknown delays.

In this section, we presented the overarching goal of this dissertation proposal to advance the state of the art in emergent mobility systems by establishing an online stochastic optimal framework for safe coordination of CAVs at different traffic scenarios, e.g., merging at roadways, intersections, roundabouts, and speed reduction zones, with imperfect state information, noisy observations, and delayed communication. We discussed three specific aims to achieve this goal, and proposed different approaches that we plan to explore for each aim. In the next chapter, we present the expected contributions of this dissertation and provide a timetable of the corresponding research tasks.

Chapter 4

EXPECTED CONTRIBUTIONS

The expected contributions of this dissertation are the following:

1. Enhancing performance and safety in coordination of CAVs in real-world scenarios, by modeling noise and uncertainties in CAVs and reformulating the coordination problem as a stochastic optimal control problem (original contribution; Aim 1).
2. Developing a decentralized framework for coordination of CAVs which rigorously incorporates noise in sensors measurements (original contribution; Aim 2).
3. Characterizing delays in communication of CAVs, and establishing a meticulous framework for coordination of CAVs under delayed communication (original contribution; Aim 3).

Our first contribution provides a useful framework for decentralized coordination of CAVs. This contribution is original since it incorporates uncertainties from the model mismatch or disturbances in the system. Although several research efforts exist for considering uncertainties in the CAV model, to the best of our knowledge, none has used a stochastic framework for coordination of CAVs, which offers significant technical challenges. The recent approach explored by Xiao et al. [66] is different from our approach since its focus is to guarantee the robustness of the deterministic solution in the presence of noise in the system. In our approach, by using the stochastic framework, we will avoid sub-optimal solutions or poor performances in the presence of uncertainties in the system [89, 104].

Our second contribution advances the state of the art in coordination of CAVs by considering noise in observations. State observations play an important role in decentralized coordination of CAVs since each CAV makes decisions based on its observations

of other CAVs' state information. Due to the noise in sensors and disturbances of the environment, this observation can be noisy. Modeling noise in our motion planning for CAVs can enhance safety in real-life scenarios.

Finally, the last contribution is of great importance with significant implications in the field of coordination of CAVs. With the advancement in communication technologies through vehicle-to-vehicle and vehicle-to-infrastructure, CAVs are able to obtain information across long distances by communicating over the wireless network. However, wireless communication networks, due to the uncertain reliability of communication links, are prone to issues such as delays [105]. Therefore, any coordination framework which neglects the effects of delays may result in failure or poor performance in practical applications. Our proposed framework will provide a practical advantage for the implementation of CAVs in real-world scenarios by considering delays in communication.

These research contributions together will result in a mathematically rigorous framework for the online coordination of CAVs in different scenarios. The proposed research will advance the state of the art in utilizing CAVs in real-world traffic scenarios to alleviate congestion, improve traffic throughput, and increase passenger safety.

Table 4.1: A provisional timetable from Spring 2020 - Fall 2020

Time Period	Research task
Spring 2020	• Modeling noise and system uncertainties in the coordination framework for CAVs. • Robust modeling of the lateral safety constraint. • Solving the problem using stochastic maximum principle. • Validating the results through simulation for an unsignalized intersection.
Summer 2020	• Reviewing the literature of the chance-constrained optimization problems • Considering the chance-constrained formulation for the soft constraints. • Validating the results through simulation for an unsignalized intersection.
Fall 2020	• Finalizing the framework for considering uncertainties and noises in the system. • Validating the result thorough experiment at UDSSC (completion of Aim 1).

Table 4.2: A provisional timetable from Winter 2020 - Winter 2021

Time Period	Research task
Winter 2020	• Reviewing the literature of the noisy measurements in the system. • Formulating the problem to incorporate noises and uncertainties in measurements.
Spring 2021	• Solving the problem of coordination of CAVs under noisy measurements. • Validating the results through simulation for an unsignalized intersection under injected noise.
Summer 2021	• Finalizing the framework for considering noisy measurements. • Validating the result thorough experiment at UDSSC (completion of Aim 2).
Fall 2021	• Reviewing the literature of decentralized systems with delays in communication. • Formulating the optimal control problem with delays in communication.
Winter 2021	• Solving the problem of coordination of CAVs with delays in communication. • Validating the results through simulation an experiment for an unsignalized intersection under imposed delays (completion of Aim 3).

Table 4.3: A provisional timetable from Winter 2020 - Winter 2021

Time Period	Research task
Spring 2022	• Finalizing the framework for the coordination of CAVs with uncertainty in the system model, noisy measurement, and delayed communication.
Summer 2022	• Defending my dissertation.

Appendix A

PUBLICATIONS

Journal Articles

1. **Chalaki, B.** and Malikopoulos, A. A., "Time-Optimal Coordination for Connected and Automated Vehicles at Adjacent Intersections," 2020 (in review).

2. Beaver, L. E., **Chalaki, B.**, Mahbub, A. M., Zhao, L., Zayas, R., and Malikopoulos, A. A., "Demonstration of a Time-Efficient Mobility System Using a Scaled Smart City," *Vehicle System Dynamics*, 2019 (in press).

Peer-Reviewed Conference Publications

1. **Chalaki, B.**, Beaver, L. E., Malikopoulos, A. A., "Experimental Validation of a Real-Time Optimal Controller for Coordination of CAVs in a Multi-Lane Roundabout," *31st IEEE Intelligent Vehicles Symposium*, 2020 (to appear).

2. **Chalaki, B.**, Beaver, L. E., Remer, B., Jang, K., Vinitsky, E., Bayen, A., and Malikopoulos, A. A., "Zero-Shot Autonomous Vehicle Policy Transfer: From Simulation to Real-World via Adversarial Learning." *International Conference on Control & Automation*, 2020 (to appear).

3. **Chalaki, B.** and Malikopoulos, A. A., "An Optimal Coordination Framework for Connected and Automated Vehicles in two Interconnected Intersections," *Proceedings of IEEE Conference on Control Technology and Applications*, pp. 888-893, 2019.

4. Jang, K., Vinitsky, E., **Chalaki, B.**, Remer, B., Beaver, L. E., Malikopoulos, A. A., and Bayen, A. , "Simulation to scaled city: zero-shot policy transfer for traffic control via autonomous vehicles," *proceedings of the 10th ACM/IEEE International Conference on Cyber-Physical Systems*, pp. 291-300, 2019.

Appendix B

COURSEWORK

Table B.1: List of coursework

	Class	Description	Term
1	MEEG 690	Intermediate Engineering Mathematics	2017 Fall
2	MATH 630	Probability Theory and application	2017 Fall
3	MEEG 698	Stochastic Optimal Control	2018 Spring
4	MEEG 620	Intermediate Dynamics	2018 Spring
5	CIEG 647	Network Optimization	2018 Spring
6	MEEG 895	Game Theory and Mechanism Design	2018 Fall
7	CIEG 646	Convex Optimization	2018 Fall
8	MEEG 890	Nonlinear Programming	2019 Spring
9	MEEG 829	Applied Nonlinear Control	2019 Spring
10	MEEG 621	Linear Systems	2019 Fall
11	MATH 631	Introduction to Stochastic Processes	2020 Spring

Appendix C

CURRICULUM VITAE

Behdad Chalaki

CONTACT INFORMATION

328 Spencer Lab
Department of Mechanical Engineering
University of Delaware
Newark, DE 19716 USA

Voice: 302–831-6576
E-mail: bchalaki@udel.edu
Website: www.sites.udel.edu/bchalaki
Others: Google Scholar, Researchgate, LinkedIn

RESEARCH INTERESTS

Optimal control, Stochastic optimal control, optimization, connected and automated vehicles, intelligent transportation system, reinforcement learning, control and robotics

EDUCATION

University of Delaware, Newark, Delaware, USA

Ph.D. Student, Mechanical Engineering, September 2022 (expected)

- Dissertation Topic: "Optimal coordination of connected and automated vehicles with uncertainty"
- Advisor: Andreas A. Malikopoulos

GPA : 3.78/4

University of Tehran, Tehran, Iran

B.Sc, Mechanical Engineering, December, 2016
GPA : 3.9/4

RELEVANT COURSES

Network optimization - Stochastic optimal control - Probability and random processes - Convex optimization - Nonlinear control - Linear systems - Nonlinear programming - Game theory and mechanism design - Advanced engineering mathematics - Intermediate dynamics - Stochastic processes

HONORS AND AWARDS

-Awarded student travel award for American control conference, 2020

-Awarded travel grant for east coast optimization meeting, George Mason University, 2020

-Awarded first place in poster presentation at MEEG graduate research showcase for prospective students, University of Delaware, 2019

-Awarded travel grant for east coast optimization meeting, George Mason University, 2019

-Graduated in the top ten percent of class and exempted from the entrance exam for graduate study, University of Tehran, 2016

-Ranked 2nd in the final project of measurement system and instrumentation course (building a prototype for pressure and temperature calibration chamber) sponsored by University of Tehran science and technology park (**$100 prize**), 2016

-Ranked 3rd among 15 finalist teams in the build of the solar water cooler (**$2,500 prize**), Iran, 2016

-Ranked 1st among 24 teams in the conceptual design of the solar water cooler, Iran, 2015

-Awarded full scholarship to study at University of Tehran for undergraduate program, 2012

-Ranked 494th among more than 300,000 participants in the nationwide universities entrance exam in mathematics and physics field for B.Sc. degree, Fall 2012

RESEARCH EXPERIENCE

University of Delaware, Newark, Delaware, USA

Research assistant, Information and Decision Science Laboratory **August, 2017 - present**

- Developing a framework for coordination of connected and automated vehicles in University of Delaware's Smart Scaled City (1:25).

- Experimental validation of different control algorithms in University of Delaware Smart Scaled City.
- Implementing and transferring the reinforcement learning policies in the scaled experimental testbed.
- Mentoring undergraduate and master students.
- Tutoring and mentoring senior design team 2018 for designing and manufacturing 25 connected autonomous vehicles (1:25).

University of Tehran, Tehran, Iran

Research assistant **May, 2016 - January, 2017**
Supervisor: Dr.Pedram Hanafizadeh

- Designing and building a solar water cooler for the national student design competition of solar cooling system.
- Thermodynamic and economic Analysis of Solar CCHP; a case study: 54 Residential Apartment Building in Kerman.

Research assistant **May, 2016 - January, 2017**
Supervisors: Dr.Ehsan Houshfar and Dr.Azadeh Jafari

- Simulation of a diesel fuel system of a gas turbine MGT-70.

Researcher, Mapfan Research Institute Magazine **August, 2015 - December, 2015**

- Conducting research related to the state of the art technologies that are utilized for harvesting energy and publishing them in the magazine.

Industry Experience

Zagross Co., Tehran, Iran
Intern in R&D section **June, 2016 - June, 2017**

- Designing and building a solar water cooler.
- Designing and building a data acquisition system for monitoring temperatures and power consumption of refrigerators.
- Developing an optimization software for water dispensers.
- Designing a defrost system for the industrial freezer and refrigerator.

Turbine Machine Middle-East Co., Tehran, Iran
Intern in R&D section **June, 2014 - September, 2014**

- Modeling gas turbine components in CATIA.
- Preparing bill of materials of components

Teaching Experience

University of Delaware, Newark, Delaware, USA
Teaching assistant

- Stochastic optimal control **Spring 2020**
- Fluid mechanics 2 **Fall 2017**
- Fluid mechanics 1 **Spring 2017**

University of Tehran, Tehran, Iran
Teaching assistant

- Optimization of thermal systems **Fall 2015**

Gam Educational Group, Tehran, Iran

Teacher and founder **September, 2012 - May, 2017**

- Teaching physics, calculus and algebra to k-12 students

Publications

Journal Articles

1. **Chalaki, B.** and Malikopoulos, A. A., "Time-Optimal Coordination for Connected and Automated Vehicles at Adjacent Intersections," 2020 (in review).
2. Beaver, L. E., **Chalaki, B.**, Mahbub, A. M., Zhao, L., Zayas, R., & Malikopoulos, A. A., "Demonstration of a Time-Efficient Mobility System Using a Scaled Smart City," *Vehicle System Dynamics*, 2019 (in press).

Peer-Reviewed Conference Publications

1. **Chalaki, B.**, Beaver, L. E., Malikopoulos, A. A., "Experimental Validation of a Real-Time Optimal Controller for Coordination of CAVs in a Multi-Lane Roundabout", *31st IEEE Intelligent Vehicles Symposium*, 2020 (to appear).
2. **Chalaki, B.**, Beaver, L. E., Remer, B., Jang, K., Vinitsky, E., Bayen, A., & Malikopoulos, A. A., "Zero-Shot Autonomous Vehicle Policy Transfer: From Simulation to Real-World via Adversarial Learning." *International Conference on Control & Automation*, 2020 (to appear).
3. **Chalaki, B.** and Malikopoulos, A. A., "An Optimal Coordination Framework for Connected and Automated Vehicles in two Interconnected Intersections," *Proceedings of IEEE Conference on Control Technology and Applications*, pp. 888-893, 2019.
4. Jang, K., Vinitsky, E., **Chalaki, B.**, Remer, B., Beaver, L. E., Malikopoulos, A. A., & Bayen, A. , "Simulation to scaled city: zero-shot policy transfer for traffic control via autonomous vehicles", *proceedings of the 10th ACM/IEEE International Conference on Cyber-Physical Systems*, pp. 291-300, 2019.

Professional Experience

Reviewer

- SAE International Journal of Connected and Automated Vehicles
- 59th IEEE Conference on Decision and Control (CDC).
- IEEE Transactions on Vehicular Technology
- 2020 IEEE IEEE Intelligent Vehicles Symposium (IV)
- 2020 IEEE Conference on Control Technology and Applications (CCTA)
- 2020 IEEE American Control Conference (ACC).
- 2019 IEEE American Control Conference (ACC).
- 14th IEEE International Conference on Automation Science and Engineering
- 58th IEEE Conference on Decision and Control (CDC).
- Vehicle System Dynamics

Seminar/Conference Presentation

- The 3rd IEEE CCTA, Hong Kong **August 19-21, 2019**
- 8th Annual Graduate Students' Forum, University of Delaware **May 10, 2019**
- East Coast Optimization Meeting, George Mason University **April 4-5, 2019**
- MEEG graduate research showcase, University of Delaware **March 14, 2019**

Organizational Affiliation

- Student member, Society for Industrial and Applied Mathematics (SIAM) **2018 - present**
- Student Member, IEEE Control Systems Society **2018 - present**
- Student Member, IEEE Young Professionals **2018 - present**
- Organizing committee member, 21st Iranian Conference on Mechanical Engineering **2013**

COMPUTER SKILLS

General : Git - LaTeX - Mathematica - MS Office Packages - Adobe Photoshop - Adobe Premiere
Operating system : Linux - Windows
Programming : MATLAB - C++ - Python - Octave
Robotics : ROS
Traffic Simulation : PreScan - PTV VISSIM
CAD : SolidWorks - AutoCad - CATIA
Data Visualization : Origin - Tecplot

LANGUAGES

Persian: Native proficiency
English: Full professional proficiency

BIBLIOGRAPHY

[1] C. G. Cassandras, "Automating mobility in smart cities," *Annual Reviews in Control*, vol. 44, pp. 1–8, 2017.

[2] B. Schrank, B. Eisele, and T. Lomax, "2019 Urban Mobility Scorecard," Texas A& M Transportation Institute, Tech. Rep., 2019.

[3] National Center for Statistics and Analysis, "Police-reported motor vehicle traffic crashes in 2018 (traffic safety facts research note.), Tech. Rep. DOT HS 812 860, November, 2019.

[4] S. Singh, "Critical reasons for crashes investigated in the national motor vehicle crash causation survey. (traffic safety facts crash stats.), Tech. Rep. DOT HS 812 506, March, 2018.

[5] L. Zhao, A. A. Malikopoulos, and J. Rios-Torres, "On the traffic impacts of optimally controlled connected and automated vehicles," in *Proceedings of 2019 IEEE Conference on Control Technology and Applications (CCTA)*. IEEE, 2019, pp. 882–887.

[6] Z. Wadud, D. MacKenzie, and P. Leiby, "Help or hindrance? the travel, energy and carbon impacts of highly automated vehicles," *Transportation Research Part A: Policy and Practice*, vol. 86, pp. 1–18, 2016.

[7] I. Klein and E. Ben-Elia, "Emergence of cooperation in congested road networks using ICT and future and emerging technologies: A game-based review," *Transportation Research Part C: Emerging Technologies*, vol. 72, pp. 10–28, 2016.

[8] S. Melo, J. Macedo, and P. Baptista, "Guiding cities to pursue a smart mobility paradigm: An example from vehicle routing guidance and its traffic and operational effects," *Research in Transportation Economics*, vol. 65, pp. 24–33, 2017.

[9] D. Tian, G. Wu, K. Boriboonsomsin, and M. J. Barth, "Performance measurement evaluation framework and co-benefit\/tradeoff analysis for connected and automated vehicles (cav) applications: A survey," *IEEE Intelligent Transportation Systems Magazine*, vol. 10, no. 3, pp. 110–122, 2018.

[10] S. E. Shladover, C. A. Desoer, J. K. Hedrick, M. Tomizuka, J. Walrand, W.-B. Zhang, D. H. McMahon, H. Peng, S. Sheikholeslam, and N. McKeown, "Automated vehicle control developments in the PATH program," *IEEE Transactions on Vehicular Technology*, vol. 40, no. 1, pp. 114–130, 1991.

[11] R. Rajamani, H.-S. Tan, B. K. Law, and W.-B. Zhang, "Demonstration of integrated longitudinal and lateral control for the operation of automated vehicles in platoons," *IEEE Transactions on Control Systems Technology*, vol. 8, no. 4, pp. 695–708, 2000.

[12] R. E. Stern, S. Cui, M. L. Delle Monache, R. Bhadani, M. Bunting, M. Churchill, N. Hamilton, H. Pohlmann, F. Wu, B. Piccoli, *et al.*, "Dissipation of stop-and-go waves via control of autonomous vehicles: Field experiments," *Transportation Research Part C: Emerging Technologies*, vol. 89, pp. 205–221, 2018.

[13] J. Lioris, R. Pedarsani, F. Y. Tascikaraoglu, and P. Varaiya, "Platoons of connected vehicles can double throughput in urban roads," *Transportation Research Part C: Emerging Technologies*, vol. 77, pp. 292–305, 2017.

[14] J. Rios-Torres, A. A. Malikopoulos, and P. Pisu, "Online Optimal Control of Connected Vehicles for Efficient Traffic Flow at Merging Roads," in *2015 IEEE 18th International Conference on Intelligent Transportation Systems*, 2015, pp. 2432–2437.

[15] J. Rios-Torres and A. A. Malikopoulos, "Automated and Cooperative Vehicle Merging at Highway On-Ramps," *IEEE Transactions on Intelligent Transportation Systems*, vol. 18, no. 4, pp. 780–789, 2017.

[16] I. A. Ntousakis, I. K. Nikolos, and M. Papageorgiou, "Optimal vehicle trajectory planning in the context of cooperative merging on highways," *Transportation Research Part C: Emerging Technologies*, vol. 71, pp. 464–488, 2016.

[17] A. M. I. Mahbub, L. Zhao, D. Assanis, and A. A. Malikopoulos, "Energy-Optimal Coordination of Connected and Automated Vehicles at Multiple Intersections," in *Proceedings of 2019 American Control Conference*, 2019, pp. 2664–2669.

[18] L. Zhao, A. A. Malikopoulos, and J. Rios-Torres, "Optimal control of connected and automated vehicles at roundabouts: An investigation in a mixed-traffic environment," in *15th IFAC Symposium on Control in Transportation Systems*, 2018, pp. 73–78.

[19] A. M. I. Mahbub, A. Malikopoulos, and L. Zhao, "Impact of connected and automated vehicles in a corridor," in *Proceedings of 2020 American Control Conference, 2020.* IEEE, 2020 (to appear).

[20] A. I. Mahbub, A. A. Malikopoulos, and L. Zhao, "Decentralized optimal coordination of connected and automated vehicles for multiple traffic scenarios," *Automatica*, vol. 117, p. 108958, 2020.

[21] A. Stager, L. Bhan, A. A. Malikopoulos, and L. Zhao, "A scaled smart city for experimental validation of connected and automated vehicles," in *15th IFAC Symposium on Control in Transportation Systems*, 2018, pp. 130–135.

[22] L. E. Beaver, B. Chalaki, A. M. Mahbub, L. Zhao, R. Zayas, and A. A. Malikopoulos, "Demonstration of a Time-Efficient Mobility System Using a Scaled Smart City," *Vehicle System Dynamics*, vol. 58, no. 5, pp. 787–804, 2020.

[23] B. Chalaki, L. E. Beaver, and A. A. Malikopoulos, "Experimental validation of a real-time optimal controller for coordination of cavs in a multi-lane roundabout," in *31st IEEE Intelligent Vehicles Symposium (to appear)*, 2020.

[24] A. A. Malikopoulos, C. G. Cassandras, and Y. Zhang, "A decentralized energy-optimal control framework for connected automated vehicles at signal-free intersections," *Automatica*, vol. 93, pp. 244–256, 2018.

[25] A. A. Malikopoulos and L. Zhao, "A closed-form analytical solution for optimal coordination of connected and automated vehicles," in *2019 American Control Conference (ACC)*. IEEE, 2019, pp. 3599–3604.

[26] A. M. I. Mahbub and A. A. Malikopoulos, "Conditions for state and control constraint activation in coordination of connected and automated vehicles," *Proceedings of 2020 American Control Conference*, 2020 (to appear).

[27] A. A. Malikopoulos, S. Hong, B. B. Park, J. Lee, and S. Ryu, "Optimal control for speed harmonization of automated vehicles," *IEEE Transactions on Intelligent Transportation Systems*, vol. 20, no. 7, pp. 2405–2417, 2019.

[28] A. A. Malikopoulos and L. Zhao, "Optimal path planning for connected and automated vehicles at urban intersections," in *Proceedings of the 58th IEEE Conference on Decision and Control, 2019*. IEEE, 2019, pp. 1261–1266.

[29] A. A. Malikopoulos, L. E. Beaver, and I. V. Chremos, "Optimal path planning and coordination for connected and automated vehicles," *arXiv:2003.12183*, 2020.

[30] A. M. I. Mahbub, V. Karri, D. Parikh, S. Jade, and A. Malikopoulos, "A decentralized time- and energy-optimal control framework for connected automated vehicles: From simulation to field test," in *SAE Technical Paper 2020-01-0579*. SAE International, 2020.

[31] J. Rios-Torres and A. A. Malikopoulos, "A survey on the coordination of connected and automated vehicles at intersections and merging at highway on-ramps," *IEEE Transactions on Intelligent Transportation Systems*, vol. 18, no. 5, pp. 1066–1077, 2016.

[32] K. Dresner and P. Stone, "Multiagent traffic management: A reservation-based intersection control mechanism," in *Proceedings of the Third International Joint Conference on Autonomous Agents and Multiagent Systems - Volume 2*, ser. AAMAS '04. Washington, DC, USA: IEEE Computer Society, 2004, pp. 530–537.

[33] ——, "A multiagent approach to autonomous intersection management," *Journal of artificial intelligence research*, vol. 31, pp. 591–656, 2008.

[34] S. Huang, A. W. Sadek, and Y. Zhao, "Assessing the mobility and environmental benefits of reservation-based intelligent intersections using an integrated simulator," *IEEE Transactions on Intelligent Transportation Systems*, vol. 13, no. 3, pp. 1201–1214, Sept 2012.

[35] T.-C. Au and P. Stone, "Motion planning algorithms for autonomous intersection management," *AAAI 2010 Workshop on Bridging The Gap Between Task And Motion Planning (BTAMP)*, pp. 2–9, 2010.

[36] A. de La Fortelle, "Analysis of reservation algorithms for cooperative planning at intersections," in *13th International IEEE Conference on Intelligent Transportation Systems*, Sept 2010, pp. 445–449.

[37] K. Zhang, D. Zhang, A. de La Fortelle, X. Wu, and J. Grégoire, "State-driven priority scheduling mechanisms for driverless vehicles approaching intersections," *IEEE Transactions on Intelligent Transportation Systems*, vol. 16, no. 5, pp. 2487–2500, Oct 2015.

[38] K. Zhang, A. De La Fortelle, D. Zhang, and X. Wu, "Analysis and modeled design of one state-driven autonomous passing-through algorithm for driverless vehicles at intersections," in *Computational Science and Engineering (CSE), 2013 IEEE 16th International Conference on*. IEEE, 2013, pp. 751–757.

[39] L. Li and F. Y. Wang, "Cooperative driving at blind crossings using intervehicle communication," *IEEE Transactions on Vehicular Technology*, vol. 55, no. 6, pp. 1712–1724, Nov 2006.

[40] F. Yan, M. Dridi, and A. E. Moudni, "Autonomous vehicle sequencing algorithm at isolated intersections," in *2009 12th International IEEE Conference on Intelligent Transportation Systems*, Oct 2009, pp. 1–6.

[41] I. H. Zohdy, R. K. Kamalanathsharma, and H. Rakha, "Intersection management for autonomous vehicles using icacc," in *2012 15th International IEEE Conference on Intelligent Transportation Systems*, Sept 2012, pp. 1109–1114.

[42] Q. Jin, G. Wu, K. Boriboonsomsin, and M. Barth, "Multi-agent intersection management for connected vehicles using an optimal scheduling approach," in *2012 International Conference on Connected Vehicles and Expo (ICCVE)*, Dec 2012, pp. 185–190.

[43] A. A.-T. Jia Wu, Florent Perronnet, "Cooperative vehicle-actuator system: a sequence-based framework of cooperative intersections management," *IET Intelligent Transport Systems*, vol. 8, pp. 352–360(8), June 2014.

[44] F. Zhu and S. V. Ukkusuri, "A linear programming formulation for autonomous intersection control within a dynamic traffic assignment and connected vehicle environment," *Transportation Research Part C: Emerging Technologies*, vol. 55, pp. 363 – 378, 2015, engineering and Applied Sciences Optimization (OPT-i) - Professor Matthew G. Karlaftis Memorial Issue.

[45] J. Wu, F. Yan, and A. Abbas-Turki, "Mathematical proof of effectiveness of platoon-based traffic control at intersections," in *16th International IEEE Conference on Intelligent Transportation Systems (ITSC 2013)*, Oct 2013, pp. 720–725.

[46] G. Raravi, V. Shingde, K. Ramamritham, and J. Bharadia, "Merge algorithms for intelligent vehicles," in *Next Generation Design and Verification Methodologies for Distributed Embedded Control Systems*. Springer, 2007, pp. 51–65.

[47] T. Awal, L. Kulik, and K. Ramamohanrao, "Optimal traffic merging strategy for communication- and sensor-enabled vehicles," in *16th International IEEE Conference on Intelligent Transportation Systems (ITSC 2013)*, Oct 2013, pp. 1468–1474.

[48] G. R. de Campos, P. Falcone, and J. Sjoberg, "Autonomous cooperative driving: a velocity-based negotiation approach for intersection crossing," in *Intelligent Transportation Systems-(ITSC), 2013 16th International IEEE Conference on*. IEEE, 2013, pp. 1456–1461.

[49] M. A. S. Kamal, J.-i. Imura, A. Ohata, T. Hayakawa, and K. Aihara, "Coordination of automated vehicles at a traffic-lightless intersection," in *Intelligent Transportation Systems-(ITSC), 2013 16th International IEEE Conference on*. IEEE, 2013, pp. 922–927.

[50] M. A. S. Kamal, J.-i. Imura, T. Hayakawa, A. Ohata, and K. Aihara, "A vehicle-intersection coordination scheme for smooth flows of traffic without using traffic lights," *IEEE Transactions on Intelligent Transportation Systems*, vol. 16, no. 3, pp. 1136–1147, 2015.

[51] P. Dai, K. Liu, Q. Zhuge, E. H.-M. Sha, V. C. S. Lee, and S. H. Son, "Quality-of-experience-oriented autonomous intersection control in vehicular networks," *IEEE Transactions on Intelligent Transportation Systems*, vol. 17, no. 7, pp. 1956–1967, 2016.

[52] M. R. Hafner, D. Cunningham, L. Caminiti, and D. Del Vecchio, "Cooperative collision avoidance at intersections: Algorithms and experiments," *IEEE Transactions on Intelligent Transportation Systems*, vol. 14, no. 3, pp. 1162–1175, 2013.

[53] J. Lee and B. Park, "Development and evaluation of a cooperative vehicle intersection control algorithm under the connected vehicles environment," *IEEE Transactions on Intelligent Transportation Systems*, vol. 13, no. 1, pp. 81–90, 2012.

[54] J. Lee, B. B. Park, K. Malakorn, and J. J. So, "Sustainability assessments of cooperative vehicle intersection control at an urban corridor," *Transportation Research Part C: Emerging Technologies*, vol. 32, pp. 193–206, 2013.

[55] D. Miculescu and S. Karaman, "Polling-systems-based control of high-performance provably-safe autonomous intersections," in *Decision and Control (CDC), 2014 IEEE 53rd Annual Conference on*. IEEE, 2014, pp. 1417–1423.

[56] I. H. Zohdy and H. Rakha, "Game theory algorithm for intersection-based cooperative adaptive cruise control (cacc) systems," in *Intelligent Transportation Systems (ITSC), 2012 15th International IEEE Conference on*. IEEE, 2012, pp. 1097–1102.

[57] J. Guanetti, Y. Kim, and F. Borrelli, "Control of connected and automated vehicles: State of the art and future challenges," *Annual reviews in control*, vol. 45, pp. 18–40, 2018.

[58] Y. Zhang and C. G. Cassandras, "Joint time and energy-optimal control of connected automated vehicles at signal-free intersections with speed-dependent safety guarantees," *arXiv preprint arXiv:1903.05692*, 2019.

[59] A. A. Malikopoulos and L. Zhao, "Decentralized optimal path planning and coordination for connected and automated vehicles at signalized-free intersections," in *58th IEEE Conference on Decision and Control*, 2019.

[60] H. Ahn, A. Colombo, and D. Del Vecchio, "Supervisory control for intersection collision avoidance in the presence of uncontrolled vehicles," in *Proceedings of the American Control Conference*, 2014.

[61] G. R. De Campos, F. Della Rossa, and A. Colombo, "Optimal and least restrictive supervisory control: Safety verification methods for human-driven vehicles

at traffic intersections," *Proceedings of the IEEE Conference on Decision and Control*, pp. 1707–1712, 2015.

[62] A. Colombo and D. Del Vecchio, "Least restrictive supervisors for intersection collision avoidance: A scheduling approach," *IEEE Transactions on Automatic Control*, 2015.

[63] H. Ahn and D. Del Vecchio, "Semi-autonomous Intersection Collision Avoidance through Job-shop Scheduling," *Proceedings of the 19th International Conference on Hybrid Systems: Computation and Control - HSCC '16*, pp. 185–194, 2016.

[64] S. A. Fayazi and A. Vahidi, "Mixed-integer linear programming for optimal scheduling of autonomous vehicle intersection crossing," *IEEE Transactions on Intelligent Vehicles*, vol. 3, no. 3, pp. 287–299, 2018.

[65] M. A. Guney and I. A. Raptis, "Scheduling-driven motion coordination of autonomous vehicles at a multi-lane traffic intersection," in *2018 Annual American Control Conference (ACC)*. IEEE, 2018, pp. 4038–4043.

[66] W. Xiao, C. G. Cassandras, and C. Belta, "Decentralized merging control in traffic networks with noisy vehicle dynamics: a joint optimal control and barrier function approach," in *2019 IEEE Intelligent Transportation Systems Conference (ITSC)*. IEEE, 2019, pp. 3162–3167.

[67] Y. Zhou, S. Ahn, M. Chitturi, and D. A. Noyce, "Rolling horizon stochastic optimal control strategy for acc and cacc under uncertainty," *Transportation Research Part C: Emerging Technologies*, vol. 83, pp. 61–76, 2017.

[68] M. P. Vitus and C. J. Tomlin, "A probabilistic approach to planning and control in autonomous urban driving," in *52nd IEEE Conference on Decision and Control*. IEEE, 2013, pp. 2459–2464.

[69] Y. Gao, F. J. Jiang, K. H. Johansson, and L. Xie, "Stochastic Modeling and Optimal Control for Automated Overtaking," in *58th Conference on Decision and Control*. IEEE, 2019, pp. 1273–1278.

[70] A. Carvalho, S. Lefévre, G. Schildbach, J. Kong, and F. Borrelli, "Automated driving: The role of forecasts and uncertainty—a control perspective," *European Journal of Control*, vol. 24, pp. 14–32, 2015.

[71] C. Liu, A. Carvalho, G. Schildbach, and J. K. Hedrick, "Stochastic predictive control for lane keeping assistance systems using a linear time-varying model," in *2015 American Control Conference (ACC)*. IEEE, 2015, pp. 3355–3360.

[72] A. Carvalho, Y. Gao, S. Lefevre, and F. Borrelli, "Stochastic predictive control of autonomous vehicles in uncertain environments," in *12th International Symposium on Advanced Vehicle Control*, 2014, pp. 712–719.

[73] A. Katriniok, S. Kojchev, E. Lefeber, and H. Nijmeijer, "A stochastic model predictive control approach for driver-aided intersection crossing with uncertain driver time delay," in *2019 18th European Control Conference (ECC)*. IEEE, 2019, pp. 243–249.

[74] D. D. Dunlap, E. G. Collins Jr, and C. V. Caldwell, "Sampling based model predictive control with application to autonomous vehicle guidance," in *Florida Conference on Recent Advances in Robotics*, 2008.

[75] K. Berntorp and S. Di Cairano, "Joint decision making and motion planning for road vehicles using particle filtering," *IFAC-PapersOnLine*, vol. 49, no. 11, pp. 175–181, 2016.

[76] K. Berntorp, T. Hoang, and S. Di Cairano, "Motion planning of autonomous road vehicles by particle filtering," *IEEE Transactions on Intelligent Vehicles*, vol. 4, no. 2, pp. 197–210, 2019.

[77] B. Chalaki and A. A. Malikopoulos, "An optimal coordination framework for connected and automated vehicles in two interconnected intersections," in *2019 IEEE Conference on Control Technology and Applications (CCTA)*. IEEE, 2019, pp. 888–893.

[78] Y. Zhang, C. G. Cassandras, and A. A. Malikopoulos, "Optimal control of connected automated vehicles at urban traffic intersections: A feasibility enforcement analysis," in *2017 American Control Conference (ACC)*. IEEE, 2017, pp. 3548–3553.

[79] M. L. Pinedo, *Scheduling: theory, algorithms, and systems*. Springer, 2016.

[80] A. A. Malikopoulos, D. N. Assanis, and P. Y. Papalambros, "Optimal engine calibration for individual driving styles," in *SAE Congress*, 2008.

[81] A. E. Bryson and Y. C. Ho, *Applied optimal control: optimization, estimation and control*. CRC Press, 1975.

[82] I. M. Ross, *A primer on Pontryagin's principle in optimal control*. Collegiate publishers, 2015.

[83] A. A. Malikopoulos and L. Zhao, "Optimal path planning for connected and automated vehicles at urban intersections," in *Proceedings of the 58th IEEE Conference on Decision and Control*, Published, (see IDS site for publication information).

[84] K. Jang, E. Vinitsky, B. Chalaki, B. Remer, L. Beaver, A. A. Malikopoulos, and A. Bayen, "Simulation to scaled city: zero-shot policy transfer for traffic control via autonomous vehicles," in *Proceedings of the 10th ACM/IEEE International Conference on Cyber-Physical Systems*, 2019, pp. 291–300.

[85] B. Chalaki, L. E. Beaver, B. Remer, K. Jang, E. Vinitsky, A. Bayen, and A. A. Malikopoulos, "Zero-shot autonomous vehicle policy transfer: From simulation to real-world via adversarial learning," in *16 th IEEE International Conference on Control & Automation (ICCA) (to appear)*, 2020.

[86] S. Thrun, M. Montemerlo, H. Dahlkamp, D. Stavens, A. Aron, J. Diebel, P. Fong, J. Gale, M. Halpenny, G. Hoffmann, K. Lau, C. Oakley, M. Palatucci, V. Pratt, P. Stang, S. Strohband, C. Dupont, L. E. Jendrossek, C. Koelen, C. Markey, C. Rummel, J. van Niekerk, E. Jensen, P. Alessandrini, G. Bradski, B. Davies, S. Ettinger, A. Kaehler, A. Nefian, and P. Mahoney, "Stanley: The robot that won the DARPA Grand Challenge," *Springer Tracts in Advanced Robotics*, 2007.

[87] M. W. Spong, S. Hutchinson, and M. Vidyasagar, "Robot Dynamics and Control Second Edition," Tech. Rep., 2004.

[88] M. Treiber, A. Hennecke, and D. Helbing, "Congested traffic states in empirical observations and microscopic simulations," *Physical review E*, vol. 62, no. 2, p. 1805, 2000.

[89] M. Athans, "The role and use of the stochastic linear-quadratic-gaussian problem in control system design," *IEEE transactions on automatic control*, vol. 16, no. 6, pp. 529–552, 1971.

[90] B. Chalaki and A. A. Malikopoulos, "Time-optimal coordination for connected and automated vehicles at adjacent intersections," *IEEE Transactions on Intelligent Transportation Systems (in review)*, 2020.

[91] K. Berntorp, T. Hoang, R. Quirynen, and S. Di Cairano, "Control architecture design for autonomous vehicles," in *2018 IEEE Conference on Control Technology and Applications (CCTA)*. IEEE, 2018, pp. 404–411.

[92] S. Peng, "A general stochastic maximum principle for optimal control problems," *SIAM Journal on control and optimization*, vol. 28, no. 4, pp. 966–979, 1990.

[93] L. Mou and J. Yong, "A variational formula for stochastic controls and some applications," *Pure and Applied Mathematics Quarterly*, vol. 3, no. 2, pp. 539–567, 2007.

[94] S. Yang, "Optimal control problem with a varying terminal time: Part i, stochastic maximum principle," *arXiv preprint arXiv:1905.03526*, 2019.

[95] A. E. Lim, J. B. Moore, and L. Faybusovich, "Separation theorem for linearly constrained lqg optimal control," *Systems & control letters*, vol. 28, no. 4, pp. 227–235, 1996.

[96] A. Lim, J. Moore, and L. Faybusovich, "Linearly constrained lq and lqg optimal control," *IFAC Proceedings Volumes*, vol. 29, no. 1, pp. 1110–1115, 1996.

[97] R. S. Bucy and P. D. Joseph, *Filtering for stochastic processes with applications to guidance*. American Mathematical Soc., 2005, vol. 326.

[98] B. D. Anderson and J. B. Moore, *Optimal filtering*. Courier Corporation, 2012.

[99] F. Berkenkamp and A. P. Schoellig, "Safe and robust learning control with gaussian processes," in *2015 European Control Conference (ECC)*. IEEE, 2015, pp. 2496–2501.

[100] L. Göllmann, D. Kern, and H. Maurer, "Optimal control problems with delays in state and control variables subject to mixed control–state constraints," *Optimal Control Applications and Methods*, vol. 30, no. 4, pp. 341–365, 2009.

[101] L. Göllmann and H. Maurer, "Theory and applications of optimal control problems with multiple time-delays," *Journal of Industrial & Management Optimization*, vol. 10, no. 2, p. 413, 2014.

[102] ——, "Optimal control problems with time delays: Two case studies in biomedicine," *Mathematical Biosciences & Engineering*, vol. 15, no. 5, p. 1137, 2018.

[103] W. Zhang, M. Tomizuka, P. Wu, Y.-H. Wei, Q. Leng, S. Han, and A. K. Mok, "A double disturbance observer design for compensation of unknown time delay in a wireless motion control system," *IEEE Transactions on Control Systems Technology*, vol. 26, no. 2, pp. 675–683, 2017.

[104] D. Bernardini and A. Bemporad, "Scenario-based model predictive control of stochastic constrained linear systems," in *Proceedings of the 48h IEEE Conference on Decision and Control (CDC) held jointly with 2009 28th Chinese Control Conference*. IEEE, 2009, pp. 6333–6338.

[105] Z. Wang, Y. Bian, S. E. Shladover, G. Wu, S. E. Li, and M. J. Barth, "A survey on cooperative longitudinal motion control of multiple connected and automated vehicles," *IEEE Intelligent Transportation Systems Magazine*, 2019.